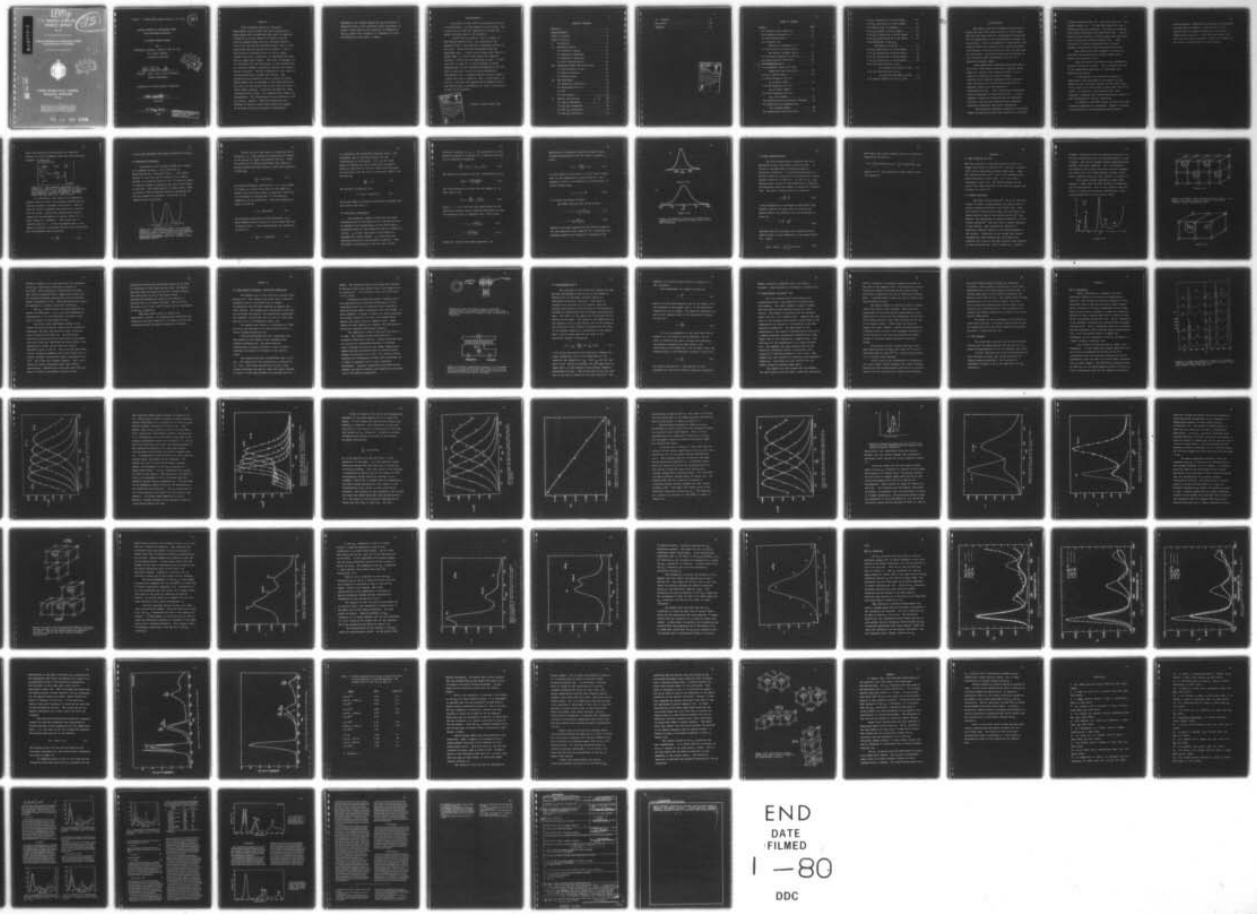
AD-A077 580 NAVAL ACADEMY ANNAPOLIS MD F/G 20/2
DIPOLAR DEFECTS IN RARE-EARTH DOPED ALKALINE-EARTH FLUORIDES. (U)
MAY 79 M K SMITH
UNCLASSIFIED USNA-TSPR-99 NL

| OF |
ADA
077 580



END
DATE
FILMED
1 -80
DDC

LEVEL II

A TRIDENT SCHOLAR PROJECT REPORT

NO. 99

DIPOLAR DEFECTS IN RARE-EARTH DOPED ALKALINE-EARTH FLUORIDES

AD A077580

DDC FILE COPY

DDC RECEIVED DEC 3 1979 E

UNITED STATES NAVAL ACADEMY
ANNAPOLIS, MARYLAND

1979

This document has been approved for public release and sale; its distribution is unlimited.

79 11 30 074

U.S.N.A. - Trident Scholar project report; no. 99 (1979)

(19)

DIPOLAR DEFECTS IN RARE-EARTH DOPED ALKALINE-EARTH FLUORIDES

A TRIDENT SCHOLAR REPORT

by

Midshipman Michael K. Smith, Class of 1979
U.S. Naval Academy
Annapolis, Maryland

DDC
RECEIVED
DEC 3 1979
E

John Fontanella

Advisor: Assoc. Prof. John Fontanella
Physics Department

Accepted for Trident Scholar Committee

C W Rector

Chairman

15 May 1979

Date

This document has been approved for public release and sale; its distribution is unlimited.

245 600

Abstract

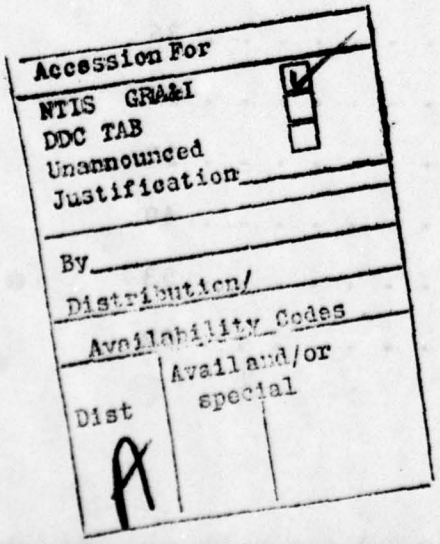
Audio frequency dielectric relaxation measurements from 5.3-380K and ionic thermocurrent measurements from 90-290K have been used to study the relaxation of dipolar defects in several calcium-fluoride samples doped with two rare-earth species. Four of the five strong relaxations that occur in rare-earth doped calcium fluoride were studied. A fit of the dielectric relaxation data for the R_I region reveals that the R_I relaxation is associated with some form of simple point defect. This site is assigned, as is consistant with the literature, to the reorientation of a nearest neighbor interstital fluorine ion around a single rare-earth. The R_{II} relaxation is also shown to be associated with a simple point defect. New relaxations are observed in the R_{II} region in doubly doped samples and are assigned to the stabilization of R_{II} sites for rare-earths that do not form this site in singly doped crystals. Activation energies for these relaxations are 0.170eV. for samarium and 0.182eV. for praseodymium. New relaxations are also observed in the R_{III} and R_{IV} regions. These new relaxations are assigned to hybrid cluster sites within the samples. On the basis of previous optical, concentration

dependence, and thermal studies the R_{III} relaxation is associated with a site containing three rare-earths, a trimer. Since only one new relaxation is observed in the R_{IV} region this relaxation is assigned to a site containing two rare-earths, a dimer.

Acknowledgment

Any effort in the realm of experimental science is a team effort. My name appears on this report. But I would like to take this opportunity to thank the people who helped make it all possible.

I would like to thank Dr. Carl G. Andeen, of Case Western Reserve Univ., for having built the apparatus used in the dielectric relaxation portion of this work. Truly excellent instruments make the experiment easy. I would like to thank Capt. Robert J. Kimble USMC, of U.S.N.A; for without his computer wizardry, I would still be analyzing my data. I would also like to thank Dr. G. Eric Matthews, of Naval Research Lab, for his invaluable assistance on the ITC part of this work, as well as many enlightening discussions. For a tremendous amount of moral support, I would also like to thank Dr. Mary C. Wintersgill, of U.S.N.A. But more than anyone else my deepest thanks and respect goes to my advisor, Dr. John J. Fontanella; he made it all possible.



Michael K. Smith, Midn. USN

TABLE OF CONTENTS

Abstract 1

Acknowledgement 3

Table of Contents 4

Index to Figures 6

I. Introduction 8

II. Relaxation Theory 11

2-1 Dielectric Theory 11

2-2 Relaxation Phenomena 14

2-3 Dielectric Relaxation 16

2-4 Ionic Thermocurrents 20

III. Lanthanide Doped Calcium-Fluoride 22

3-1 The Structure of CaF_2 22

3-2 Defect Structure 22

3-3 Previous Work 25

IV. The Experiment 29

4-1 Dielectric Relaxation 29

4-2 Determination of ε'' 32

4-3 ITC 34

4-4 ITC Analysis 36

V. Results and Analysis 37

5-1 The R_I Relaxation 37

5-2 The R_{II} Relaxation 40

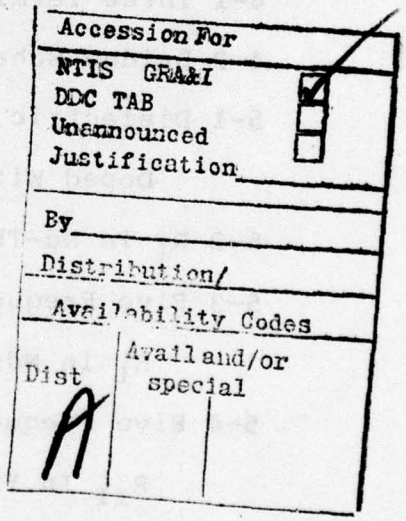
5-3 The R_{III} Relaxation 53

5-4 The R_{IV} Relaxation 62

VI. Summary 76

References 78

Appendix 81



INDEX TO FIGURES

Figure — Page

2-1 Parallel Plate Capacitor 12

2-2 Frequency Dependence of ε' 13

2-3 The Bistable Model 14

2-4 Frequency and Temperature Dependence of ε'' 19

3-1 Pure Calcium Fluoride Lattice and Nearest Neighbor Defect 24

3-2 Dielectric Spectrum of CaF_2:Er 23

4-1 Three Terminal Electrode 31

4-2 Bridge Schematic 31

5-1 Dielectric Spectra for CaF_2 Doped With Each Rare-Earth 38

5-2 R_I in Nd-Tb Sample 39

5-3 Five Frequency Plot for R_I in Nd-Tb Sample 41

5-4 Five Frequency Plot for R_{II} In Yb-Ho Sample 43

5-5 Five Frequency Plot for R_{II} in Ho Sample 45

5-6 Determination of Activation Enthalpy . . 46

5-7 Modified Five Frequency Plot for Ho doped Sample 48

5-8 Inequivalent Potential Wells 49

5-9 R_{II} Relaxations in Er-Sm Sample 50

5-10 R_{II} Relaxations in Tm-Pr Sample 51

5-11 Several R_{II} Site Models 54

5-12 R_{III} Region in Yb-Ho Sample 56

5-13 R_{III} Relaxations in Tm-Tb Sample . . . 58

5-14 R_{III} Relaxations in Er-Sm Sample . . . 59

5-15 Broadening of the R_{III} Relaxation in CaF_2:Er 61

5-16 R_{IV} Relaxations in Er-Sm Sample 63

5-17 R_{IV} Relaxations in Nd-Tb Sample 64

5-18 R_{IV} Relaxations in Nd-Dy Sample 65

5-19 R_{IV} Relaxations in Tm-Tb Sample 66

5-20 ITC Identification of R_{IV} for Smaller Rare-Earth: Er-Sm . . 69

5-21 ITC Identification of R_{IV} for Smaller Rare-Earth: Nd-Tb . . 70

5-22 Several Models for the R_{IV} Site 75

Introduction

The defect structure of doped calcium-fluoride (CaF_2) has come under close scrutiny in recent years. This has come about both for technological reasons and for the advancement of the understanding of defects in ionic solids. From the standpoint of application, CaF_2 crystals doped with elements of the Lanthanide series (rare-earths), as well as uranium, have long been used as laser hosts. Rare-earth doped calcium-fluoride is also currently under consideration for use in a capacitive pressure gauge.

Many experimental techniques have been used in the study of the defect structure of CaF_2:Re, among these are: electron spin resonance (ESR), (1,2,3) anelastic relaxation,(4) nuclear magnetic resonance,(5,6) optical absorption,(7,8) selective laser excitation,(9) ionic thermocurrents,(10,11) Mossbauer effect,(12) and dielectric relaxation(3,13,14). Also, significant theoretical work has been done in this field (15,16). In this research, dielectric relaxation was the technique utilized, with the ionic thermocurrent technique providing significant additional information.

The dielectric relaxation spectrum of rare-earth doped calcium-fluoride has been measured as a function

of dopant concentration,(13) rare-earth type,(14) and thermal history (7). In each case significant new information has been obtained. From previous research five strong relaxations have been noted (14). One of these has been labled R_I and correlates well with the A site of selective excitation studies (9). This relaxation is usually associated with a nearest neighbor interstitial charge compensating fluorine.

Many models have been proposed to account for the other four relaxations including simple point defects and clusters (14,17).

Some theoretical calculations have attempted to describe clustering (15,16). But it remains the task of the experimental physicist to investigate and describe this system.

In the present work dielectric relaxation measurements have been made on six samples of CaF_2 doped with two rare-earth species (Er-Sm 0.05%, Tm-Pr 0.01%, Tm-Tb 0.3%, Nd-Dy 0.05%, Yb-Ho 0.05%, and Nd-Tb 0.05%). In addition, ionic thermocurrent "peak cleaning" techniques have proved particularly useful in the investigation of the R_{IV} relaxation.

In chapter 2 the basic theory of dielectrics and relaxation phenomena are discussed. Chapter 3 contains an introduction to the Lanthanide doped calcium-

fluoride system. Experimental procedures and apparatus are described in chapter 4. The results of this research and the analysis techniques utilized are summarized in chapter 5. The conclusions drawn from this work are found in chapter 6 along with suggestions for further investigation into this system.

Chapter 2

2-1 Dielectric Theory

A dielectric is, by definition, an insulator. That is to say, there are no free charge carriers to conduct current when an electric field is applied. The response of a dielectric to an applied electric field is governed by two parameters: the real part of the dielectric constant (ε'), which is related to the polarization of the dielectric, and the complex part of the dielectric constant (ε''), which is related to the energy dissipated during the polarization.

The capacitance of a system is given by:

$$C = \frac{Q}{V} \qquad 2\text{-}1$$

where Q is the charge stored, V is the voltage across the capacitor and C is the capacitance of the system. If the capacitor is a perfect parallel plate capacitor, as shown in figure 2-1, the capacitance is given by:

$$C_0 = \frac{\varepsilon_0 A}{d} \qquad 2\text{-}2$$

Where A is the area of the plates, d is the spacing between them and ε_0 is the permittivity of free space.

If a dielectric is inserted between the plates and an electric field applied, charge within the dielectric will tend to reorient with the applied field. This charge alignment will tend to compensate for the charge on the plates and therefore will reduce the voltage across the system. By equation 2-1 this reduction in voltage will result in an increase in the total capacitance of the system by a factor ε' so that:

$$C = \varepsilon' C_0 \qquad 2\text{-}3$$

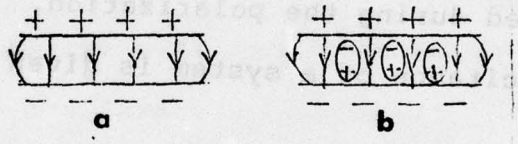


Fig. 2-1(a). shows the configuration of a parallel plate capacitor. Fig 2-1(b) shows the charge reorientation within a dielectric when a field is applied.

The charge alignment within a dielectric may be due to many mechanisms. These include the reorientation of ions within the dielectric, the reorientation of permanent dipoles, and the preferential orientation of the electrons around each atom. At low frequencies the dielectric constant is governed by all three mechanisms. In the intermediate frequency range only

ionic and electronic contributions are important. Finally, in the UV frequency range only the electronic alignment is important.

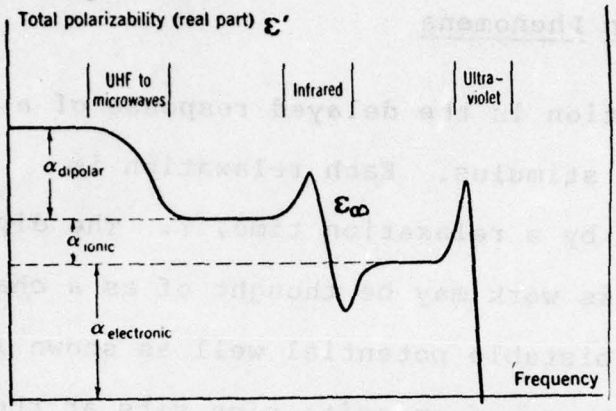


Figure 2-2. The frequency dependence of the dielectric constant (ε') showing the various types of polarization. (From Introduction to Solid State Physics, edited by C. Kittel. New York: John Wiley and Sons Inc., 1971, p.461)

In a dielectric, when there is no externally applied electric field, the permanent dipoles will be oriented randomly throughout the material. When an external field is applied, the dipoles will reorient with the field. During this reorientation process energy will be dissipated in a manner similar to I R power losses in a conductor. This power loss is characterized by σ". σ" will be proportional to the number of dipoles reorienting and the energy dissipated per reorientation and is given by:

$$\sigma'' = \frac{Gd}{A} \qquad 2\text{-}4$$

$\varepsilon''=\sigma''/\omega\varepsilon_0$ and represents the power dissipated per cycle.

2-2 Relaxation Phenomena

Relaxation is the delayed response of a system to an applied stimulus. Each relaxation is characterized by a relaxation time, τ. The dipoles studied in this work may be thought of as a charge sitting in a bistable potential well as shown in figure 2-3 where a charge of opposite sign sits at the center of the well. The dipole may be in either state. When an electric field is placed across the dielectric and the well depths are modified, transitions to the enhanced well are favored.

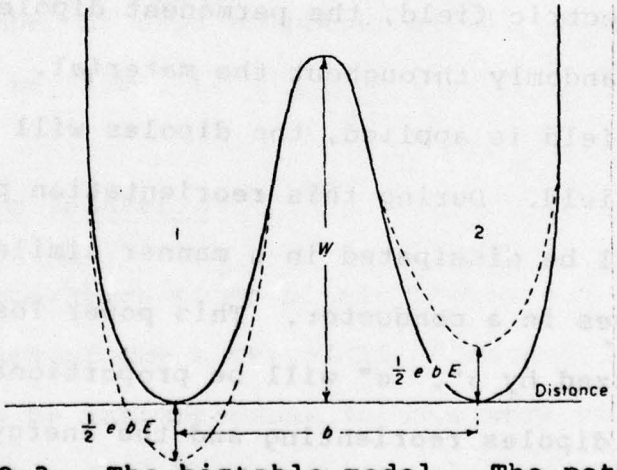


Figure 2-3. The bistable model. The potential energy as a funtion of distance has two minima, "potential wells," whose depth has been modified by an electric field. (From V.V. Daniel in Dielectric Relaxation, New York: Academic Press, Inc.,1967, p.21.)

Within the well each dipole is vibrating with a frequency, f_0. Each oscillation represents an attempt by the dipole to "jump" the potential barrier. Since the system is in thermal equilibrium, the number of dipoles having sufficient energy to make the transition is given by:

$$\frac{N}{N_0} = \exp(-E/kT) \qquad 2\text{-}5$$

the Maxwell-Boltzmann distribution. N_0 is the number of dipoles in a given state and N is the number of dipoles with sufficient energy to make the transition. k is Boltzmann's constant and T is the absolute temperature of the dielectric. Thus the frequency of jumps is given by:

$$f = f_0 \exp(-E/kT) \qquad 2\text{-}6$$

By examining transitions in both directions, for a small applied electric field, it can be shown that the relaxation time, τ, that characterizes the relaxation, is given by:

$$\tau = \frac{1}{2f} = \tau_0 \exp(E/kT) \qquad 2\text{-}7$$

τ_0 is known as the reciprocal frequency factor. The relaxation time is the time constant for the reorientation of the dipoles. If N_0 is the total number of dipoles that will orient with an applied electric field and N is the net number that have made the transition then the rate of transition, dN/dt, will be given by:

$$\frac{dN}{dt} = - \frac{N}{\tau} \qquad 2\text{-}8$$

The solution of equation 2-8:

$$N = N_0 [1 - \exp(-t/\tau)] \qquad 2\text{-}9$$

gives the number of dipoles preferentially aligned with the field at any time, t.

2-3 Dielectric Relaxation

The relaxation times of electronic and ionic relaxations are of the order of 10^{-10} seconds and will be assumed to be instantaneous in this work since a reasonable value for the relaxation time of a dipole is 10^{-6}sec. ϵ_s is the real part of the dielectric constant for a static field. ϵ_∞ is the ionic and electronic portion of the dielectric constant. Thus the dipolar contribution to the real part of the

dielectric constant is $\varepsilon_s - \varepsilon_\infty$. The polarization of the permanent dipoles in a dielectric is found by solution of the differential equation:

$$\tau \frac{dP_D}{dt} + P_D(t) = (\varepsilon_s - \varepsilon_\infty)E(t) \qquad 2\text{-}10$$

The solution of equation 2-10 for a sinusoidal E(t) is:

$$P_D^*(t) = \frac{(\varepsilon_s - \varepsilon_\infty)E(t)}{1 + i\omega\tau} \qquad 2\text{-}11$$

The total dielectric constant for the system, ε^*, is then found to be:

$$\varepsilon^* - \varepsilon_\infty = \frac{P_D^*}{E(t)} = \frac{\varepsilon_s - \varepsilon_\infty}{1 + i\omega\tau} \qquad 2\text{-}12$$

Since $\varepsilon^* = \varepsilon' - i\varepsilon''$, the real and complex parts of the dielectric constant may be found by separating the real and imaginary parts of equation 2-12. This yields:

$$\varepsilon' = \varepsilon_\infty + \frac{\varepsilon_s - \varepsilon_\infty}{1 + \omega^2\tau^2} \qquad 2\text{-}13$$

$$\varepsilon'' = \frac{(\varepsilon_s - \varepsilon_\infty)\omega\tau}{1 + \omega^2\tau^2} \qquad 2\text{-}14$$

These are known as the Debye equations. An

application of Boltzmann statistics between sites aligned preferentially with the field or against it gives:

$$\varepsilon_s - \varepsilon_\infty = \frac{NP^2}{3\varepsilon_0 kT} = \alpha_D \qquad 2\text{-}15$$

N is the dipole concentration, p is the dipole moment and T is the temperature of the dielectric. This parameter, known as the dielectric polarizability, is further broken down:

$$\varepsilon_s - \varepsilon_\infty = \alpha_D = \frac{A}{T} \qquad 2\text{-}16$$

A is called the dipole strength.

The Debye equations may now be written:

$$\varepsilon' = \varepsilon_\infty + \frac{A}{T(1 + \omega^2\tau^2)} \qquad 2\text{-}17$$

$$\varepsilon'' = \frac{A\omega\tau}{T(1 + \omega^2\tau^2)} \qquad 2\text{-}18$$

Equation 2-18 when coupled with the defining equation for the relaxation time, equation 2-7, constitutes the governing equation for dielectric relaxations (18).

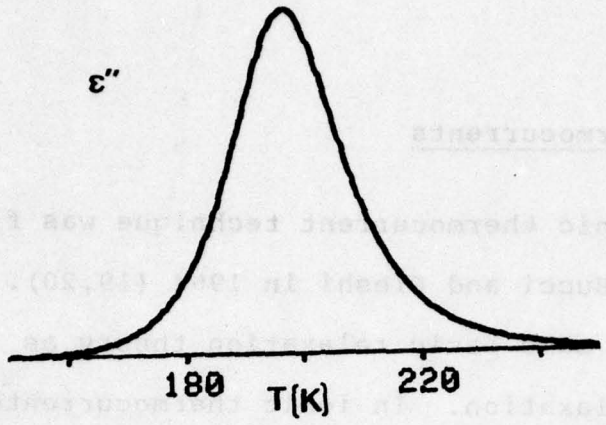


Figure 2-4a

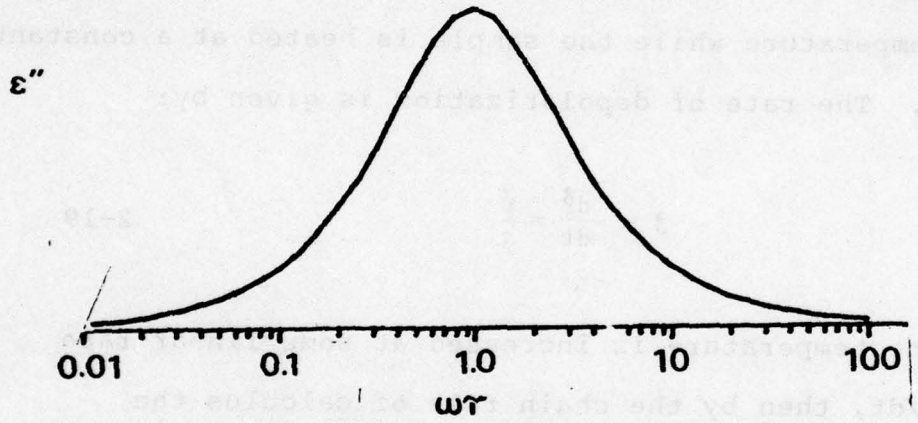


Figure 2-4b

Figure 2-4a shows ε" plotted as a function of temperature and figure 2-4b shows how ε" varies with frequency.

2-3 Ionic Thermocurrents

The ionic thermocurrent technique was first developed by Bucci and Fieshi in 1964 (19,20). It relies on the same basic relaxation theory as dielectric relaxation. In ionic thermocurrents the dipoles within the dielectric are polarized by a static electric field for a time $t>>\tau$, so that $P = \alpha_D$. The depolarization current is then measured as a function of temperature while the sample is heated at a constant rate. The rate of depolarization is given by:

$$j = -\frac{d\vec{P}}{dt} = \frac{\vec{P}}{\tau} \qquad 2\text{-}19$$

If the temperature is increased at some linear rate $b=dT/dt$, then by the chain rule of calculus the depolarization and therefore the current density is given by:

$$\vec{j} = \frac{\vec{P}}{\tau} = -b\frac{d\vec{P}}{dt} \qquad 2\text{-}20$$

By separating the variables and integrating from T where $P_0 = P(T_0)$ to any temperature T and substituting for τ gives:

$$\ell N(\vec{P}) - \ell N(\vec{P}_0) = -\frac{1}{b\tau_0}\int_{T_0}^{T} \exp(-E/kT)\,dT \qquad 2\text{-}21$$

And finally the current density $j=\vec{j}\cdot\hat{n}$ as a function of temperature is given by:

$$j(t) = \frac{P_0}{\tau_0} \exp(-E/kT)\exp\{-(b\tau_0)^{-1} \int_{T_0}^{T} \exp(-E/kT)dT\} \quad \text{2-22}$$

where $P = \vec{P} \cdot \hat{n}$. This equation is often known as the "ITC Equation."

Chapter 3

3-1 The Structure of CaF_2

The basic structure of calcium-fluoride is that of a simple cubic array of fluorine (F^-) ions with a calcium (Ca^{2+}) ion at the center of every other cube. Thus the lattice cations (Ca^{2+}) form a face centered cubic array containing a cubic array of F^- ions. This represents a unit cell. The length between Calcium ions in the [100] direction is the lattice constant and is equal to 5.46 Å (21).

3-2 Defect Structure

The ionic radius of the Ca^{2+} ion in the fluorite lattice (1.26 Å) is approximately the same as that of triply ionized rare-earths (1.06-1.28 Å) (22). Thus CaF_2 crystals may be easily grown with rare-earth ions substituted for some of the lattice cation Ca^{2+} ions. However, the replacement of doubly ionized Ca^{2+} ions by triply ionized Re^{3+} ions will leave a charge imbalance in the lattice. This requires the addition of additional negative charge to the system somewhere in the lattice. Originally it was thought that charge compensation takes place by way of an additional fluorine ion in one of the body centered sites adjacent to the rare-earth ion. This is known as a "nearest

neighbor" interstitial and the resultant rare-earth and fluorine interstitial pair is sometimes known as a Type I dipole. The nearest neighbor charge compensated site exhibits tetragonal symmetry. (For a discussion of site symmetry and crystal directions see the reference for figure 2-2) This configuration is shown, along with a diagram of the pure CaF_2 lattice, in figure 3-1.

This simple charge compensation model would explain a single peak for both dielectric relaxation and ITC measurements. This is not, however, the case. Figure 3-2 shows the dielectric spectrum for a CaF_2 crystal doped with the rare-earth, Erbium.

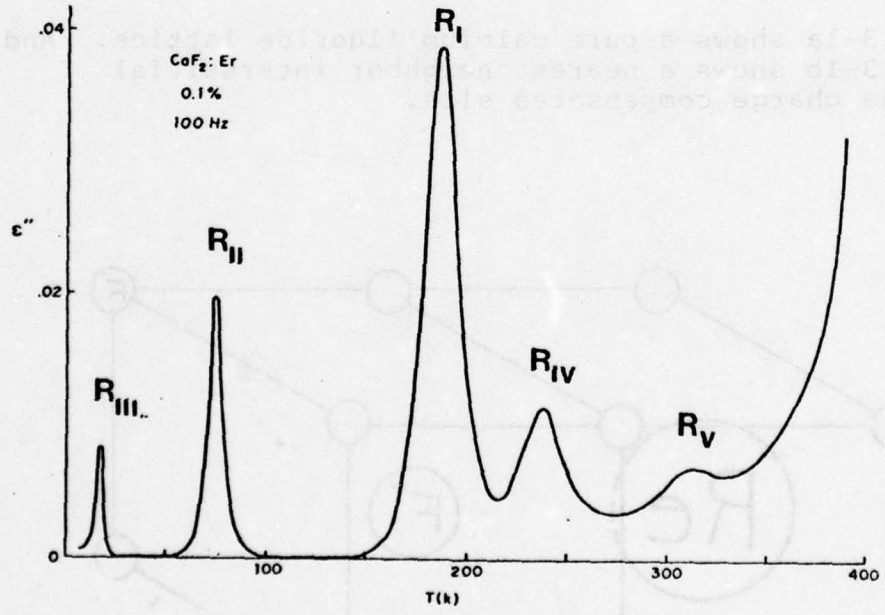


figure 3-2

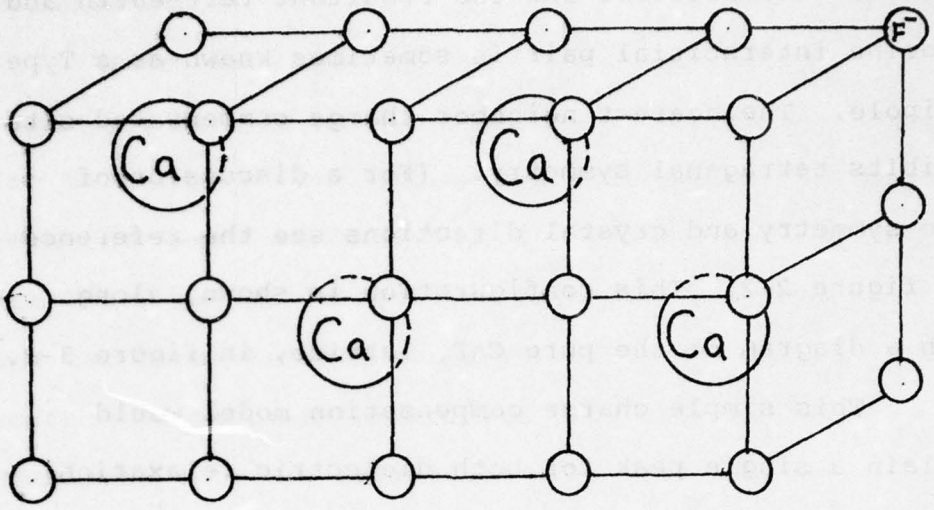


Figure 3-1a

Figure 3-1a shows a pure calcium fluoride lattice. And figure 3-1b shows a nearest neighbor interstitial fluorine charge compensated site.

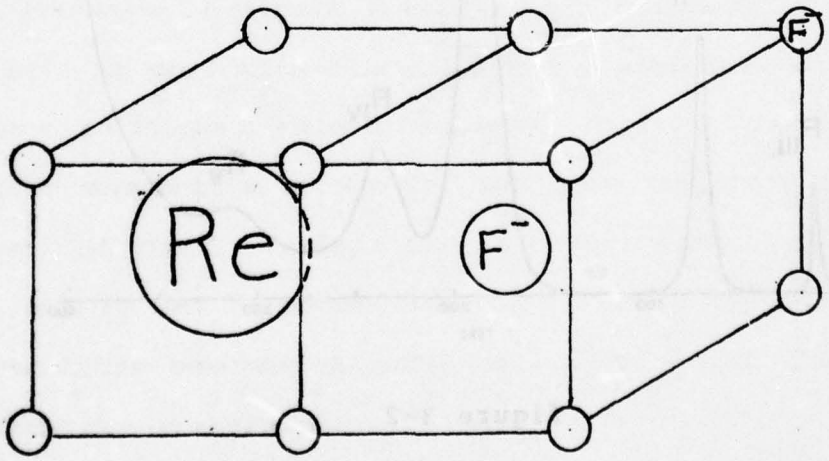


Figure 3-1b

Multiple relaxations have also been observed using ITC (17). Clearly, then, more than one type of dipolar defect occurs in $CaF_2:Re^{3+}$.

Two other types of charge compensation were proposed in early work on $CaF_2:Er^{3+}$. One, is that of a next nearest neighbor interstitial, also known as a Type II dipole. It consists of an F^- ion occupying the body centered site along the [111] axis from the rare-earth. This site exhibits trigonal symmetry. The other proposed site is a non-locally compensated site that exhibits cubic symmetry. The charge compensating F^- ion is located elsewhere in the lattice. This site would have no dipole moment and would be "invisible" to dielectric relaxation and ITC.

3-3 Previous Work

The first observation of a dielectric relaxation in rare-earth doped CaF_2 was reported in 1970 by Franklin and Marzulo (24). The relaxation was observed in $CaF_2:Gd^{3+}$ and had an activation energy of 0.4eV. This relaxation corresponds to the R_I relaxation mentioned earlier and was correlated to a tetragonal ESR center that had been identified in previous work (1). Consequently, this relaxation was associated with a nearest neighbor interstitial F^- ion charge

compensation.

Stott and Crawford first observed the R_{II} relaxation in 1970 by means of the ITC technique. They also found the R_{I} relaxation and by relating the dipole concentrations for the R_{I} and R_{II} relaxations, correlated the R_{II} relaxation to a weak trigonal site that had been observed using ESR (23). Stott and Crawford tentatively identified this site as being associated with the relaxation of a next nearest neighbor interstitial F^- ion. This identification was later disputed by Franklin et al. on the basis of ESR studies, and, in a later work, Crawford et al. agreed with the idea that the R_{II} relaxation was not caused by a next nearest neighbor interstitial (4,25). In the same paper Crawford et al. identified a new relaxation at about 230K, R_{IV}, and suggested that this relaxation was the type II dipole (next nearest neighbor). ITC studies of strontium-fluorides doped with rare-earths seemed to support this assignment (25,26). Another factor supporting this model was that the activation energy of the R_{IV} relaxation is higher than that of the R_{I}, and it was believed that the F^- ion would relax through the nearest neighbor site. This left the R_{II} relaxation unexplained.

In more recent years, the dielectric relaxation

studies of Andeen et al. have show that the assignment of the R_{IV} relaxation to the type II dipole is incorrect. The relaxation is significantly broader than would be expected from a simple point defect and its strength increases monotonically with increasing dopant concentration (13). These characteristics would be expected of a cluster associated relaxation.

The R_{III} relaxation has only been observed by Andeen and Fontanella. Due to its high dependence on concentration it is also believed to be due to some form of cluster of rare-earths (13,14).

One of the most significant studies of the defect structure of CaF_2:Re, other than by relaxation techniques, has been the selective laser excitation work of Tallant and Wright (9). By selectively exciting the optically active electrons of the dopant rare-earth they have identified two point defect sites (designated A and B) and at least two cluster associated sites (C and D). The A site has been shown to have tetragonal symmetry and is most likely due to a nearest neighbor interstitial charge compensated site (23). The B site has trigonal symmetry. The C and D sites are cluster associated since they exhibit upconversion. Upconversion occurs when more than one atom at a defect site absorbs a photon during

excitation and then the excitation energy of one atom is transfered to the other excited atom. The photon that will then be given off will be of higher energy then those used to excite the defect sites. Upconversion between two simple point defects is possible but it is highly unlikely. The C site is believed to be a lower order cluster and may correspond to the R_{IV} relaxation.

Thus many models exist to explain the experimental results. By studying CaF_2 doped with two different rare-earth species it is hoped to elicit new information about the defect structure of CaF_2:Re.

Chapter 4

4-1 Experimental Procedure: Dielectric Relaxation

The samples used in this work were obtained from Optovac Inc. The crystals were grown under a fluorine atmosphere and are relatively free of oxygen contamination that has been observed in samples from other sources. The dopants were introduced to the melt as rare-earth fluorides at the concentration specified. The crystals, as received, were in 2.54 cm. disks that had been cut to a thickness of about 2 mm.

The samples were ground to a thickness of 1.5mm. and were then polished to an optical quality using 1 micron diamond polishing paste.

Aluminum electrodes were then evaporated onto the surface of the samples in the standard three terminal configuration. The three terminal configuration is shown in figure 4-1 and is used to eliminate the effects of fringing of the electric field.

The evaporations were accomplished under a bell jar. The system was first evacuated to a pressure of 10 torr. Then Argon gas was bled in and a high-voltage discharge was used to clean the sample surfaces to assure a solid bond between the electrode and the

sample. The insulating gap on the sample was achieved by placing a thin steel shadow ring on the sample prior to evaporation. The insulating rings were each about .01 mm. thick.

Conductance divided by angular frequency (G/ω) and capacitance were measured isothermally at five frequencies from 100 to 10,000 Hz using a specially modified General Radio transformer ratio arm bridge. A basic schematic is shown in figure 4-2. After balancing the bridge, values for G/ω and C are automatically punched onto paper tape for computer input. These values are then inputed to a computer for conversion to dielectric constants and further analysis.

The temperature range in this work was from 5.3 to 380K. The temperature was maintained in a Cryogenics Associates cryostat. Liquid helium was used for cooling for temperatures between 5.3 and 80K; liquid nitrogen was used for all higher temperatures. Temperature was controlled using an electric heater capable of delivering up to 16W. The control circuit consisted of a Wheatstone's bridge with a platinum (30 to 380K) or germanium (5.3 to 30K) resistance thermometer. Integral, proportional and differential feedback was used to maintain the temperature to within .01K of the desired temperature.

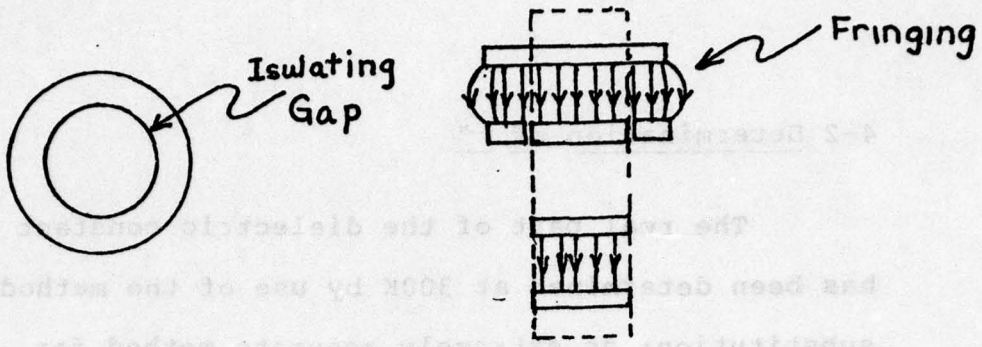


Figure 4-1 shows the three terminal electrode configuration. By measuring only across the center section, the effects of electric field fringing may be neglected.

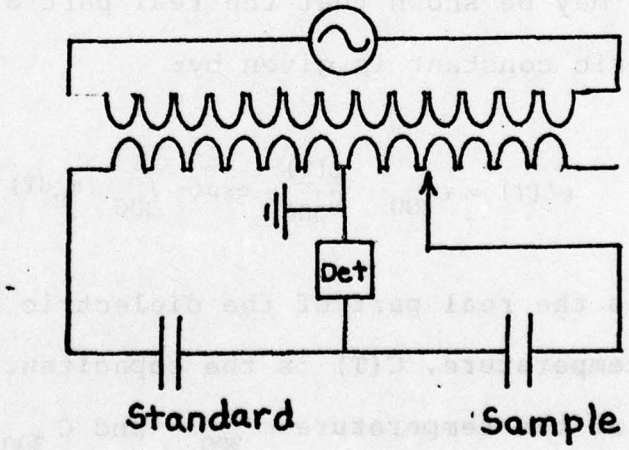


Figure 4-2 shows a simplified schematic of the bridge. When the tap has been positioned so that the voltage across the detector is zero, the bridge is said to be balanced and the data may be recorded.

4-2 Determination of ε"

The real part of the dielectric constant for CaF_2 has been determined at 300K by use of the method of substitution; an extremely accurate method for determining dielectric constants. This value is assumed to be the same for all samples, since the dipolar contribution to the real part of the dielectric constant is insignificant for the dopant concentrations used. The effect of the impurities on the host lattice should also be small. The change in the capacitance of the samples is due to two factors: one is the change in the real part of the dielectric constant and the other is the thermal expansion or contraction of the sample. Thus it may be shown that the real part of the dielectric constant is given by:

$$\varepsilon'(T) = \varepsilon'_{300} \frac{C(T)}{C_{300}} \exp\left(-\int_{300}^{T} \alpha_p dT\right) \qquad 4\text{-}1$$

$\varepsilon'(T)$ is the real part of the dielectric constant at a given temperature, C(T) is the capacitance of the sample at the temperature ε'_{300} and C_{300} are the real part of the dielectric constant and the capacitance at 300K, and α_p is the isobaric linear thermal expansion coefficient for CaF . The values used are for pure CaF due to the lack of values for the doped material. The

exponent is evaluated using numerical integration in 10K increments.

The conductance of a sample is given by:

$$G = \frac{\sigma A}{d} \qquad 4\text{-}2$$

where A is the cross-sectional area of the sample, d is the thickness of the sample, and σ is the dielectric conductivity of the sample. By combining equations 2-4 and 4-2 the imaginary part of the dielectric constant is given by:

$$\varepsilon'' = \frac{Gd}{\varepsilon_0 \omega A} \qquad 4\text{-}3$$

All of the parameters on the right hand side of equation 4-3 are known or can be measured. But in order to eliminate the error involved with measuring the geometric properties of the crystal, the capacitance of the system (eq. 2-2) is used so that the imaginary part of the dielectric constant is given by:

$$\varepsilon'' = \frac{\varepsilon' G}{\omega C} \qquad 4\text{-}4$$

The values obtained for ε'' may then be fit with equations 2-7 and 2-18 to obtain values for activation

energy, reciprocal frequency factor and dipole strength. These methods are discussed in chapter five.

4-3 Experimental Procedure: ITC

The ionic thermocurrent measurements were accomplished using a Cary Model 401 vibrating reed electrometer. The sample chamber is made of copper, with the heating wires cemented around the lower portion. The sample is insulated from the grounded copper base by a thin sapphire disk. Sapphire was used since it has extremely high thermal conductivity at low temperatures and because of its excellent electrical insulation properties. The measurement of the temperature of the sample is accomplished by the use of a copper-constantan thermocouple imbedded into a CaF_2 sample that is also mounted on a sapphire disk. The reference for the thermocouple is a liquid nitrogen bath. The samples, the same crystals used for the dielectric relaxation portion of this work, were cleaved to a thickness between 0.5 and 1.0 mm. The samples were then measured to determine exact geometric properties. Electrodes are then painted onto the samples using an aluminum powder paint.

The samples are then loaded into the chamber. The high-voltage electrode used to apply the polarizing

field is attached to a painted aluminum electrode on the face of the sapphire disk. Good electrical contact between the sample electrodes and the high-voltage electrode is assured by the use of additional aluminum paint. A spring loaded contact was used to detect the depolarizatiom current.

The sample chamber is contained within a vacuum tight, thin-walled brass cylinder. The electrical connections for the polarization, measurement of the depolarization current and for temperature control are fed through stainless steel tubes attached at the top of the sample chamber. These tubes also serve to support the sample chamber. During the measurement of a depolarization current a one atmosphere pressure of dry helium gas is bled into the cylinder and sample chamber to minimize thermal gradients within the system.

Polarization fields of about 8kV/m were used. Peak depolarization currents were about 10^{-14} A with a backround-noise of about 10^{-16} A. Linear heating rates of 3 to 5K/min. were employed.

Initial cooling was accomplished by submerging the entire sample holder assembly into liquid nitrogen. Heating was then accomplished by the use of an electric heater that was controlled by a system that compares

the actual thermo-couple voltage to a generated reference. The reference utilized was a third order approximation to the thermo-couple voltage output. A voltage ramp input to the controller generates the desired linear heating rate. The thermo-couple voltage approximation is good to within $\pm$0.3K. The error varies slowly and therefore has little effect on the linearity of the heating rate. The controller will maintain the sample temperature to within $\pm$0.1K of the desired temperature.

The output of the electrometer is recorded on a strip chart recorder. At several times during the ITC run temperatures from the thermo-couple were recorded to assure a linear heating rate.

4-4 ITC Analysis

The strip chart recorder plot is then digitized manually and the depolarization currents are fit to a numerical approximation of the ITC equation (Eq. 2-22).

The most important use of the ITC method was the peak cleaning technique that allows resolution of closely spaced relaxations. This technique is discussed in chapter 5 as it was applied to the R_{IV} relaxation.

Chapter 5

The R_I Relaxation

The R_I relaxation is, possibly, the best understood relaxation in rare-earth doped calcium fluoride. This relaxation has been correlated to the tetragonal site in EPR and rotational Zeeman studies. The R_I relaxation is fairly independent of rare-earth type as can be seen in figure 5-1 where the relaxation spectra for CaF_2 crystals doped with 0.1 mol-% of each of the rare-earths are plotted (14). The R_I relaxation is the dominant relaxation for crystals with low dopant concentrations. The R_I relaxation also first increases and then decreases with increasing dopant concentration (13). This information tends to support the assignment, in the literature, of the R_I relaxation to a type I dipolar relaxation (24).

The results of this work tend to support this assignment. In this reguard the sample doped with 0.05 mol-% each of neodymium and terbium is the most interesting since the activation energies of the two relaxations cause the peaks to be more widely separated than in other samples. The dielectric relaxation data, at 1000 Hz, for the Tb-Nd sample is shown in figure 5-2 with a theoretical curve and the expected constituent

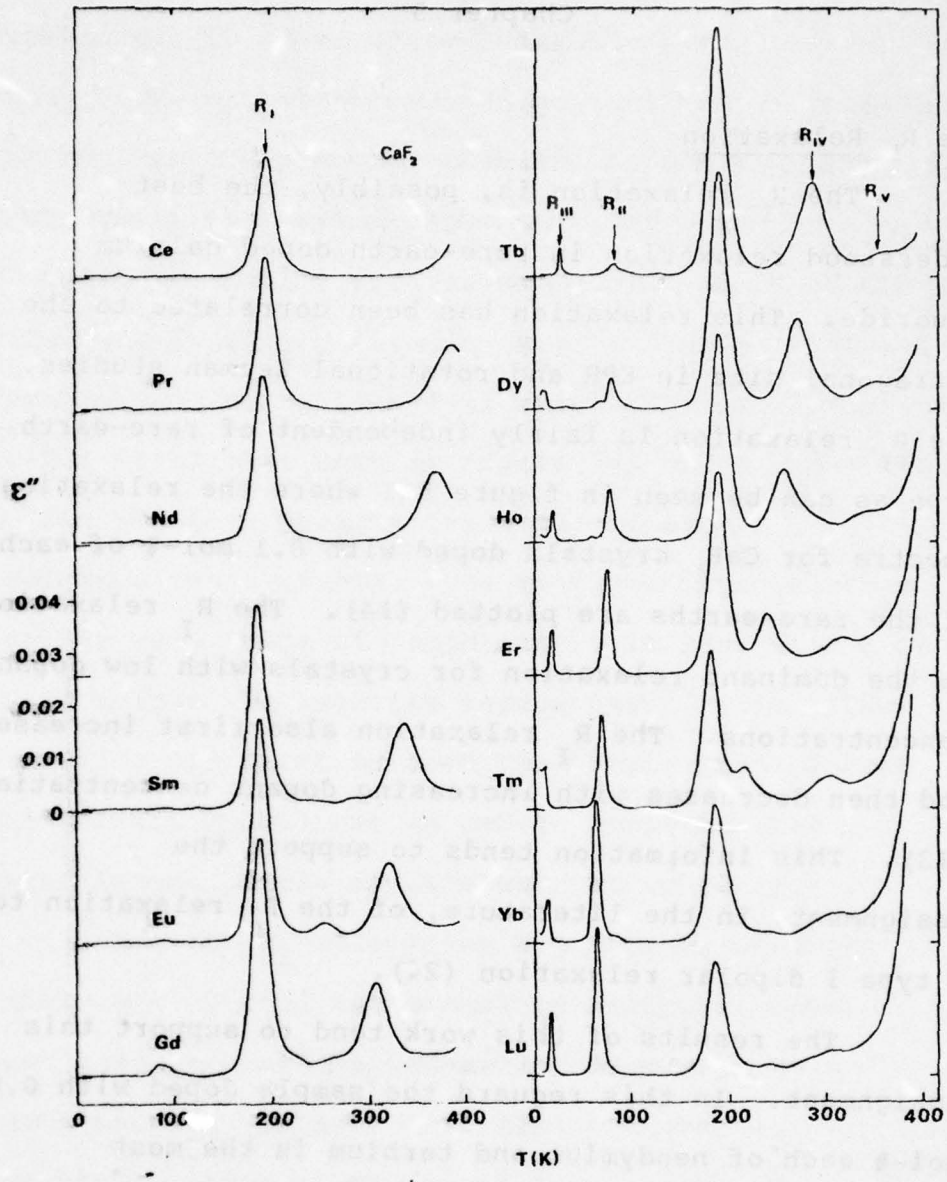


Figure 5-1 shows the dielectric spectra for calcium-fluoride crystals doped with 0.1 mol-% of each of the rare-earths. (From reference #14)

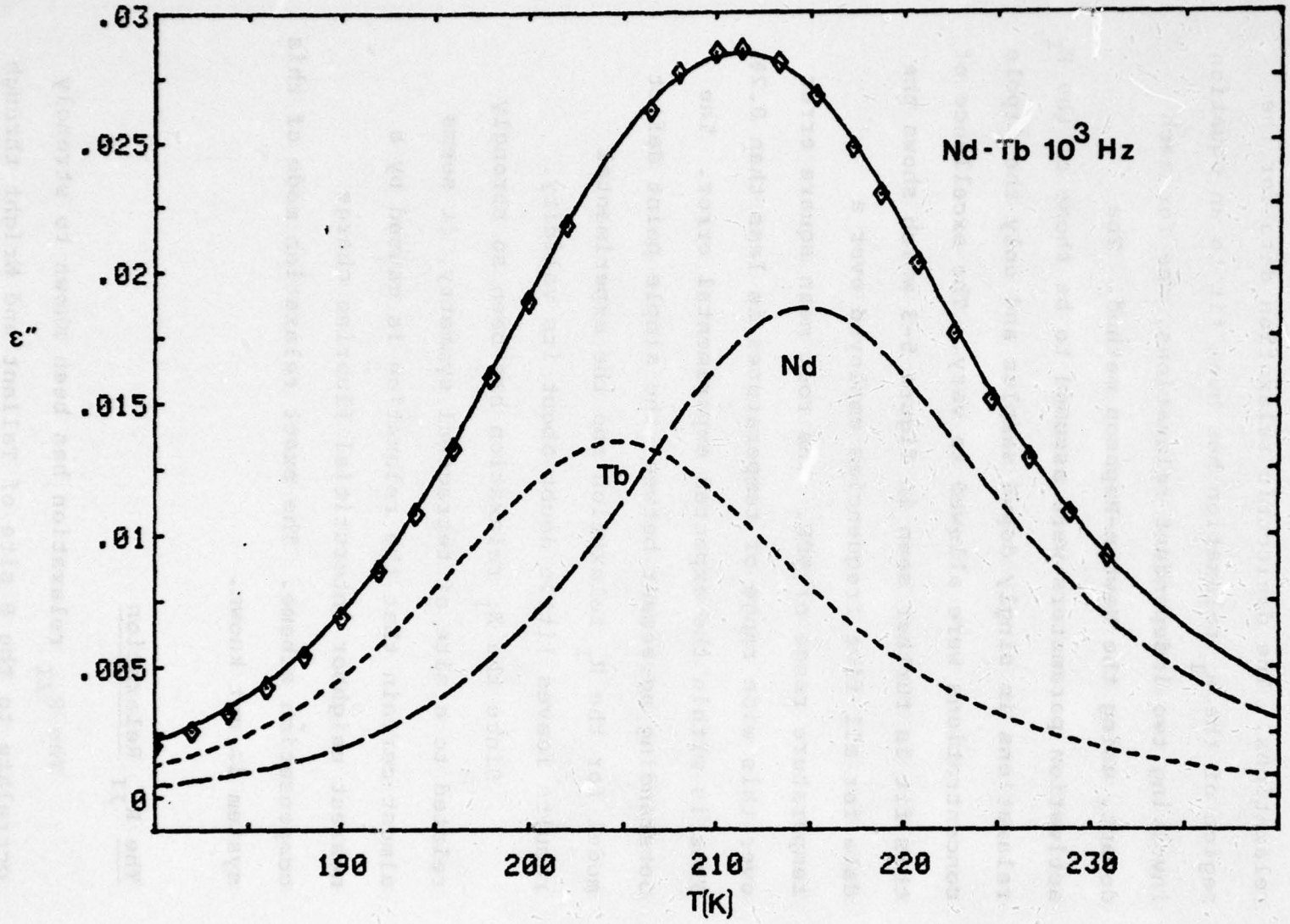


Figure 5-2 shows the data for the Nd-Tb sample. The solid line is a fit to this data using the simple point defect model.

relaxations. The dielectric relaxation data for the region of the R_I relaxation has been fit to an equation involving two independent relaxations, one for each dopant, using the Newton-Raphson method. The activation parameters were assumed to be those of the R_I relaxations in singly doped samples and only the dipole concentrations were allowed to vary. The excellence of this fit is further seen in figure 5-3 which shows the data for all five frequencies employed over a temperature range of 90K. The root mean square error over this wide range of temperatures is less than 0.2%. This is within the expected experimental error. The outstanding agreement between the simple point defect model for the R_I relaxation and the experimental results leaves little doubt about its validity.

Since the R_I relaxation has been so strongly related to a site of tetragonal symmetry, it seems almost certain that the relaxation is caused by a nearest neighbor interstitial fluorine charge compensation scheme. The exact relaxation mode of this system is not known.

The R_{II} Relaxation

The R_{II} relaxation has been shown to strongly correlate to the B site of Tallant and Wright through

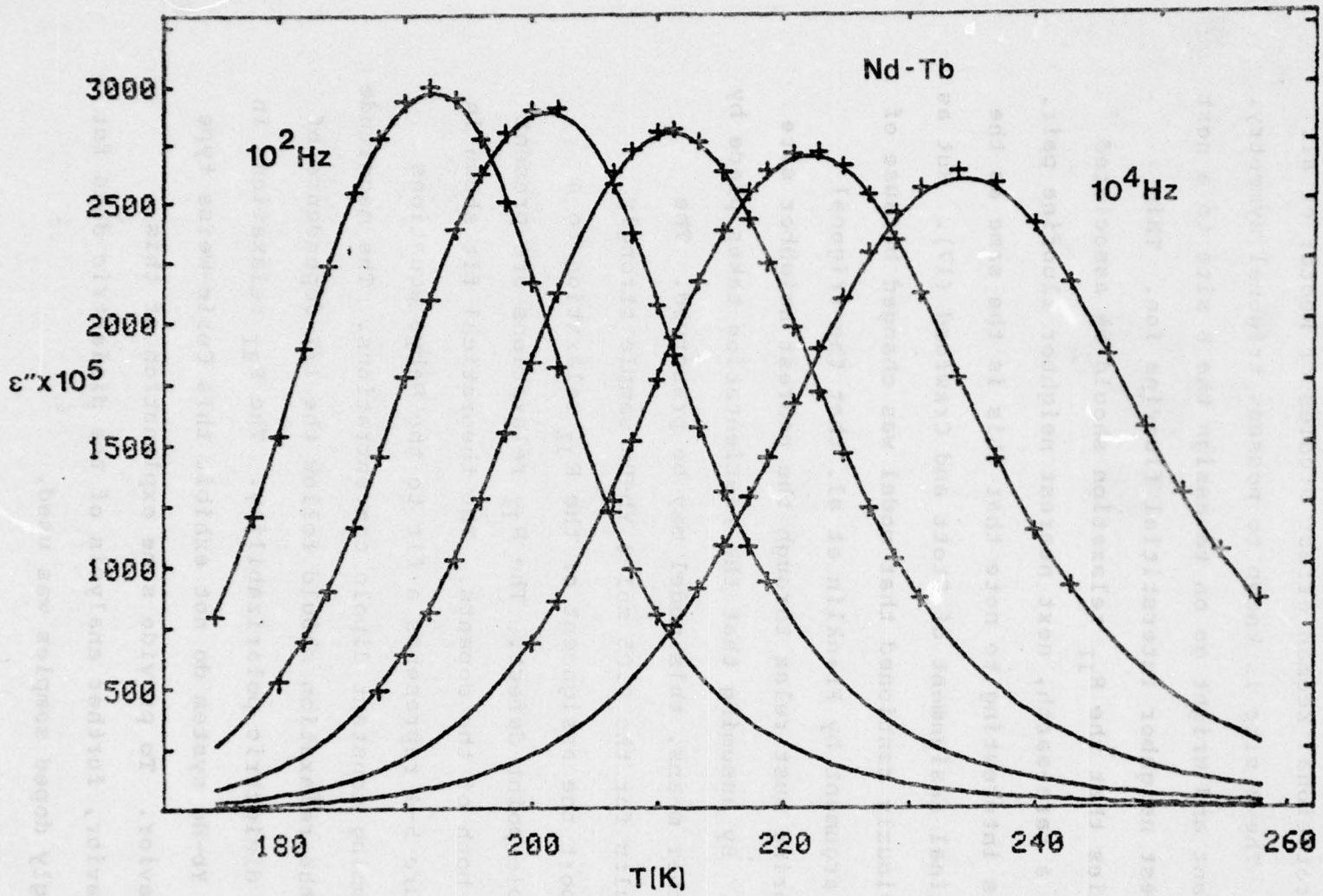


Figure 5-3 shows the data for the Nd-Tb sample fit to the simple point defect model, at all five frequencies.

the rotational Zeeman effect studies of Rector et al. (7). The B site is known to possess trigonal symmetry. Tallant and Wright go on to assign the B site to a next nearest neighbor interstitial fluorine ion. This implies that the R_{II} relaxation should be associated with a rare-earth, next nearest neighbor fluorine pair. It is interesting to note that this is the same as the original assignment of Stott and Crawford (17). But as previously mentioned that model was changed because of the argument by Franklin et al. that the trigonal fluorine must relax through the nearest neighbor site (4). By assuming that the reorientation takes place by another means, this model may be preserved. The results for the 0.05 mol-% Yb-Ho sample strongly support the assignment of the R_{II} relaxation to a simple point defect. The R_{II} relaxations are present for both of the dopants. The theoretical fit shown in figure 5-4 represents a fit to the Debye equations assuming constant dipole concentrations. The magnitude of the relaxation should follow the 1/T dependence of the dielectric polarizability. The R_{II} relaxations in the Yb-Ho system do not exhibit this Curie-Weiss type behavior. To provide some explanation of this behavior, further analysis of the dielectric data for singly doped samples was used.

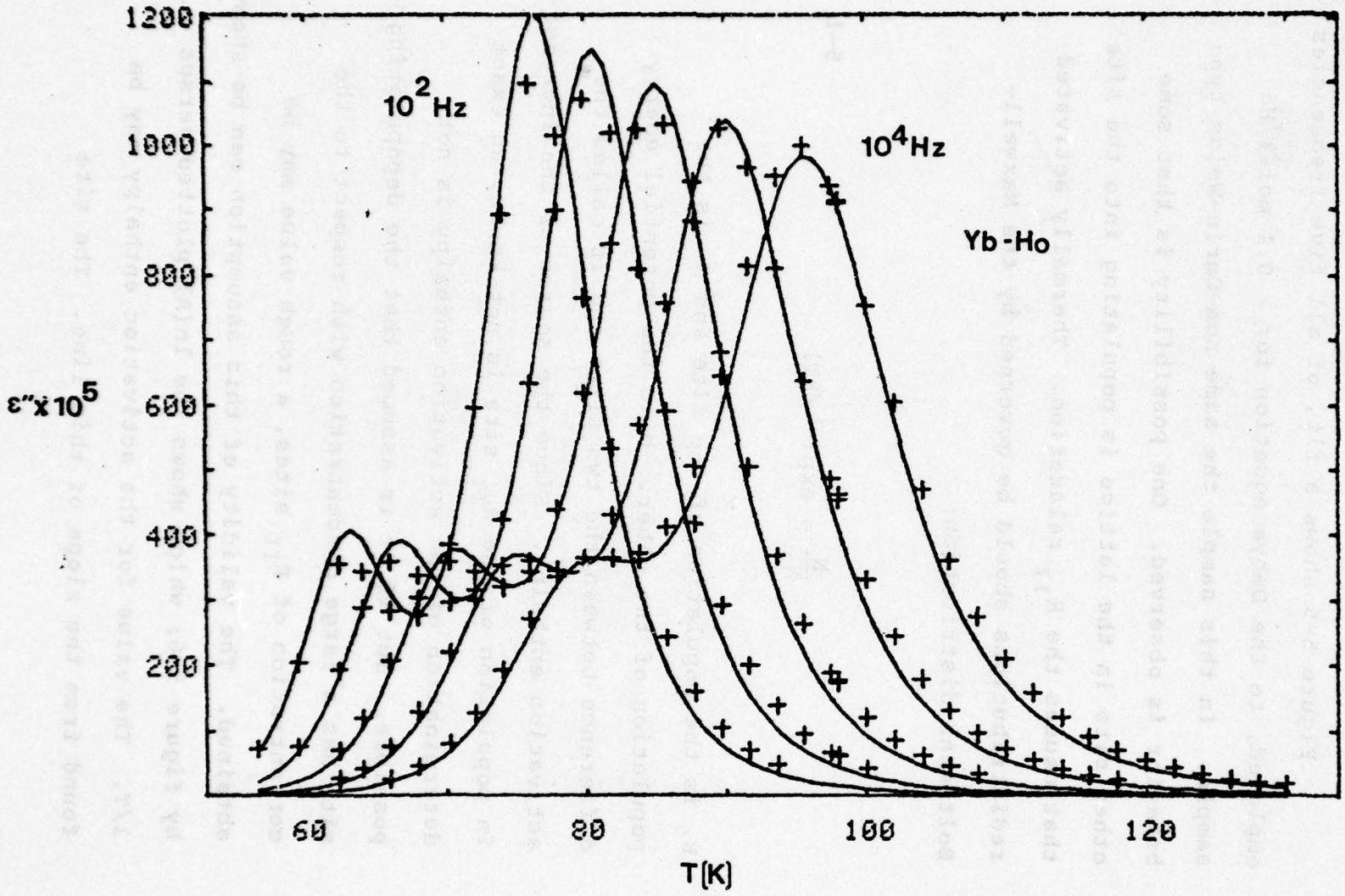


Figure 5-4 shows the data for the Yb-Ho sample fit with the simple point defect model. Notice that the relaxation does not follow the 1/T behavior of the theoretical curve.

Figure 5-5 shows a fit, of all five frequencies employed, to the Debye equation for a 0.1 mol-% Ho sample. In this sample the same non-Curie-Weiss type behavior is observed. One possibility is that some other site in the lattice is populating into the site that causes the R_{II} relaxation. Thermally activated redistributions should be governed by the Maxwell-Boltzmann distribution:

$$\frac{N}{N_0} = \exp(-h/kT) \qquad 5\text{-}1$$

N_0 is the population of one site and N is the population of the other. h is the potential energy difference between the two sites and is called the activation enthalpy. Since the source of the increase in population of the R_{II} site is not known, an exact determination of the activation enthalpy is not possible. But if it is assumed that the depopulating site has a large concentration with respect to the concentration of R_{II} sites, a rough value may be obtained. The validity of this assumption can be shown by figure 5-6; which shows the ln(A) plotted versus 1/T. The value for the activation enthalpy may be found from the slope of this line. The site

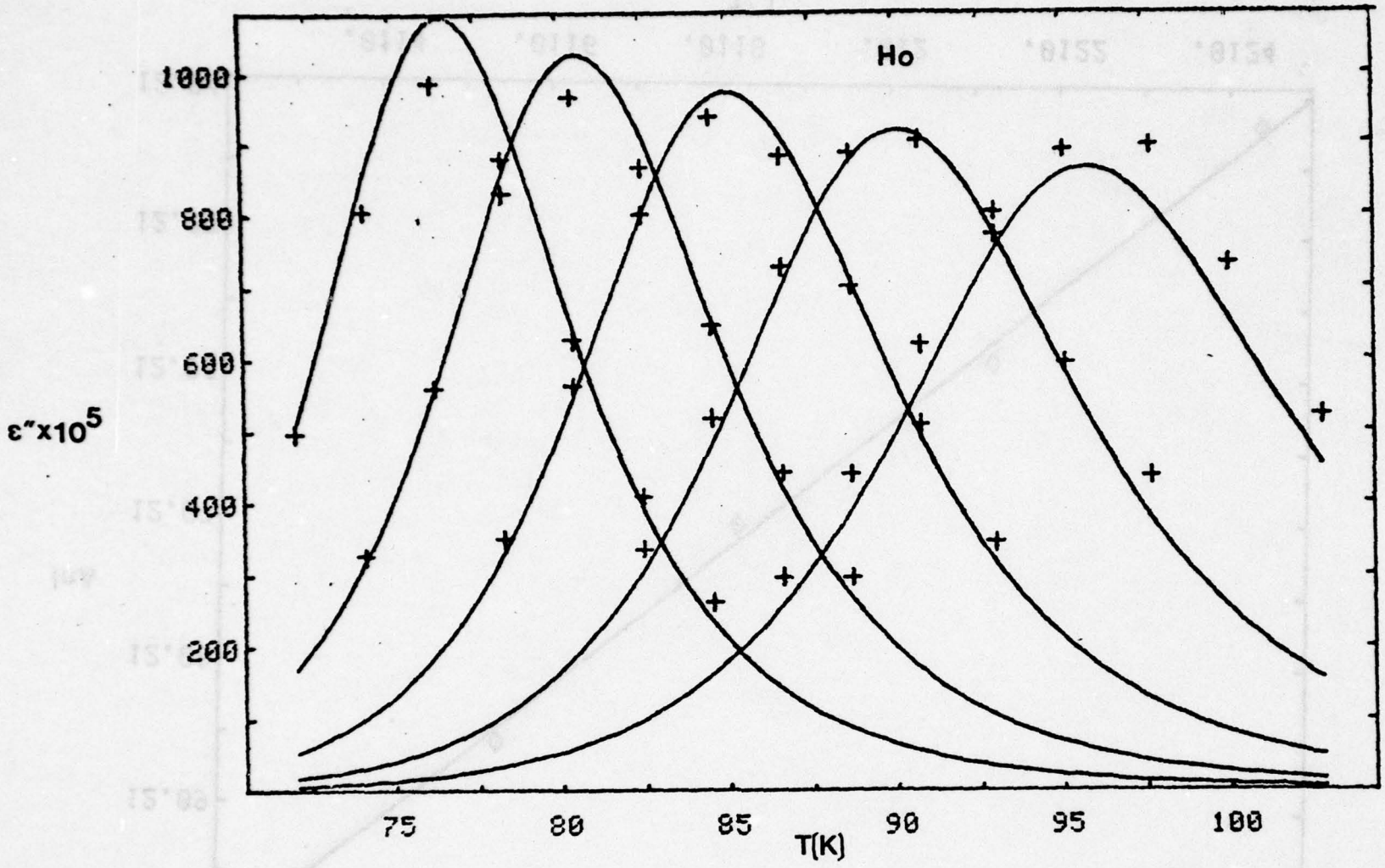


Figure 5-5 shows the data for a sample doped only with Ho. Notice that the same non-Curie-Weiss type behavior is observed.

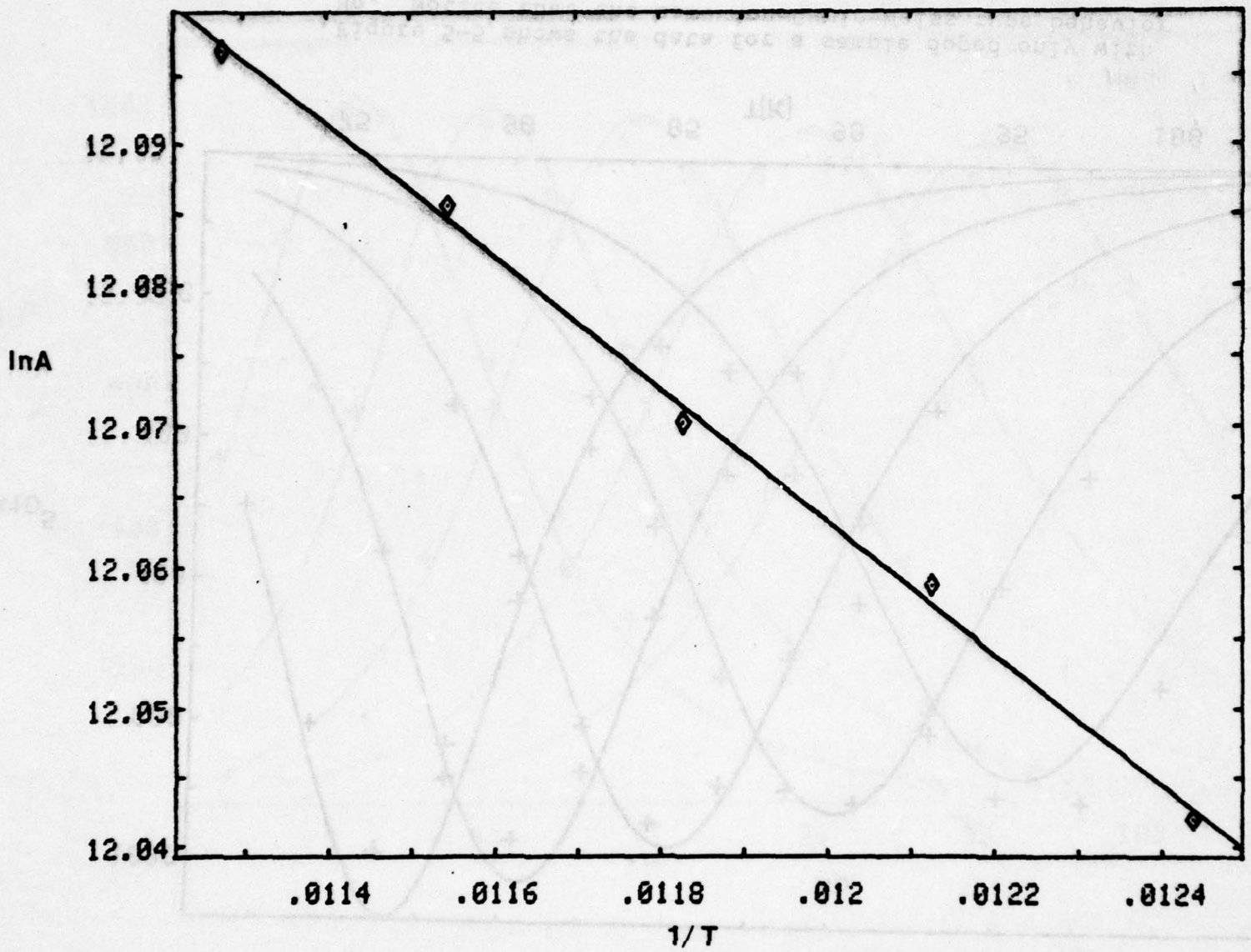


Figure 5-6 shows the natural log of the dipole strength versus 1/T for the Ho doped sample.

inequivalency is about 0.004 eV. The result of fitting the the 0.1% Ho data to the Debye equation, modified so that A=A exp(-h/kT), is shown in figure 5-7.

The activation enthalpy for each of the R_{II} relaxations is found to decrease with decreasing dopant ion size for singly doped samples. This is to be expected since this represents a favoring of the R_{II} site by samples doped with smaller rare-earths which has already been shown.

It can be seen in figure 5-7 that even with the addition of the thermal population of the R_{II} site, the theoretical fit is not within expected experimental error. This suggests that the relaxation time might not be governed by equation 2-7. A different model which may account for all of the observed effects is that the R_{II} relaxation takes place between two slightly nonequivalent potential wells. One such model has been predicted, theoretically, by Catlow (15). He suggests that the R_{II} relaxation represents a transition between nearest neighbor and next nearest neighbor sites. This model will explain most of the dielectric relaxation results for R_{II}. The potential as a function of position for this model is shown in figure 5-8.

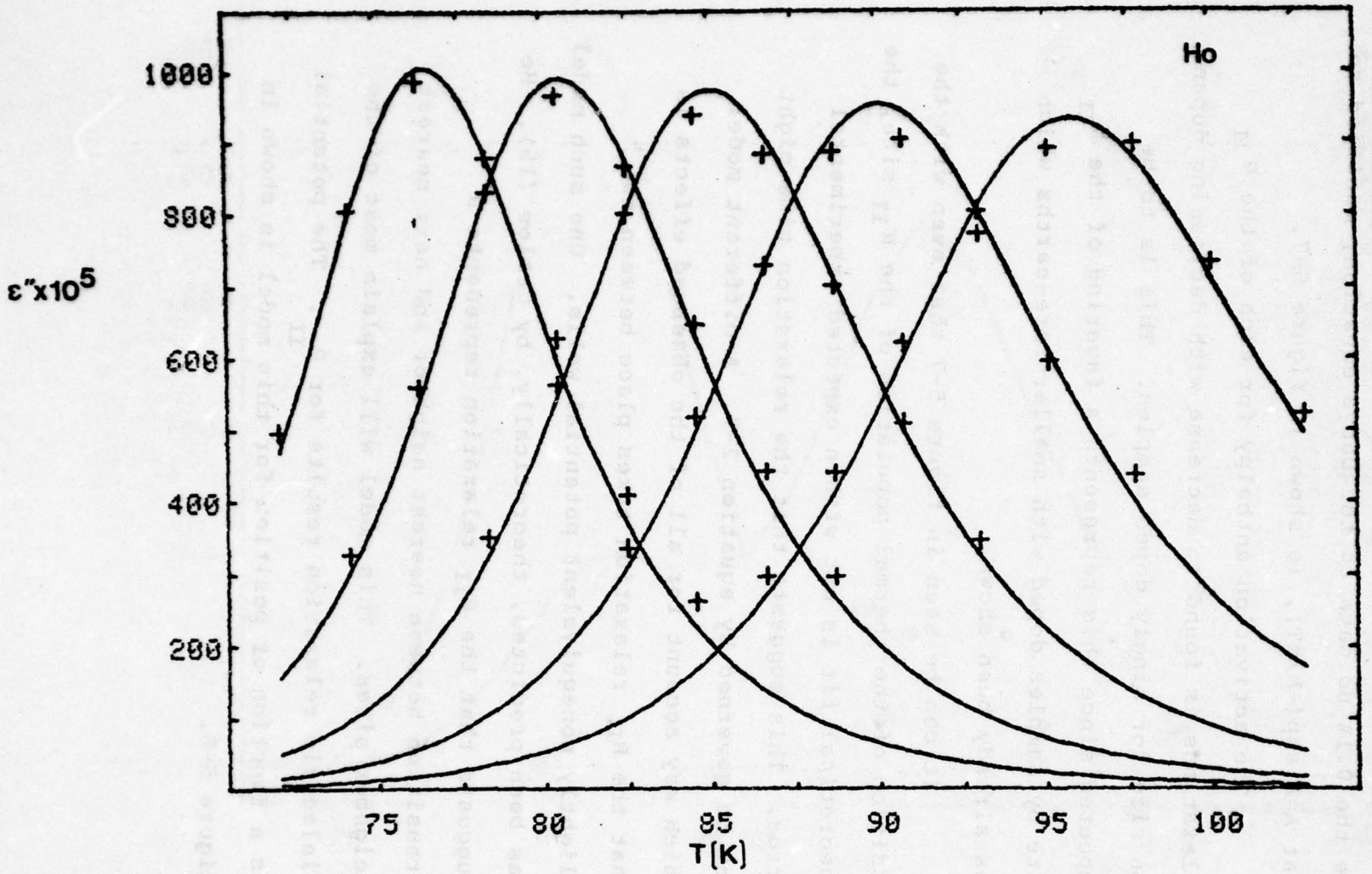


Figure 5-7 shows the Ho doped sample data fit with a curve that accounts for the thermal population of the site.

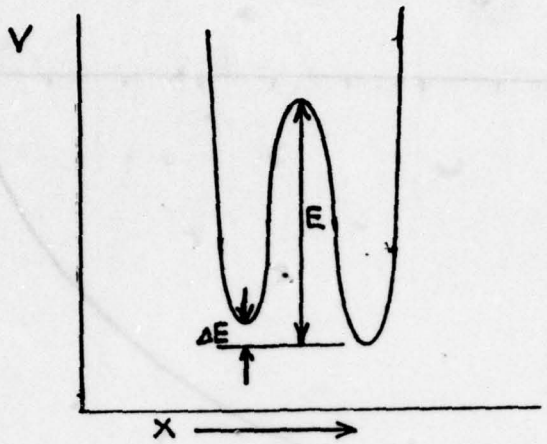


Figure 5-8 shows the potential as a function of position for the predicted nearest neighbor next nearest neighbor transition.

Unfortunatly, the inequivalent sites are nearest neighbor and next nearest neighbor and consequently this model cannot account for recent annealing results (7).

The Yb-Ho system was the only sample studied where a strong R_{II} relaxation is present in both singly doped samples for dopants used. Interesting results are also found in samples doped with 0.05 mol-% each erbium and samarium and 0.01 mol-% thulium and praseodymium. These results are shown in figures 5-9 and 5-10. The relaxation for the smaller rare-earth is present, as expected, and a new relaxation is found at a higher temperature. The activation energy of the new relaxation in the Er-Sm system is .170 eV and the activation energy for the new peak in Tm-Pr is .182 eV.

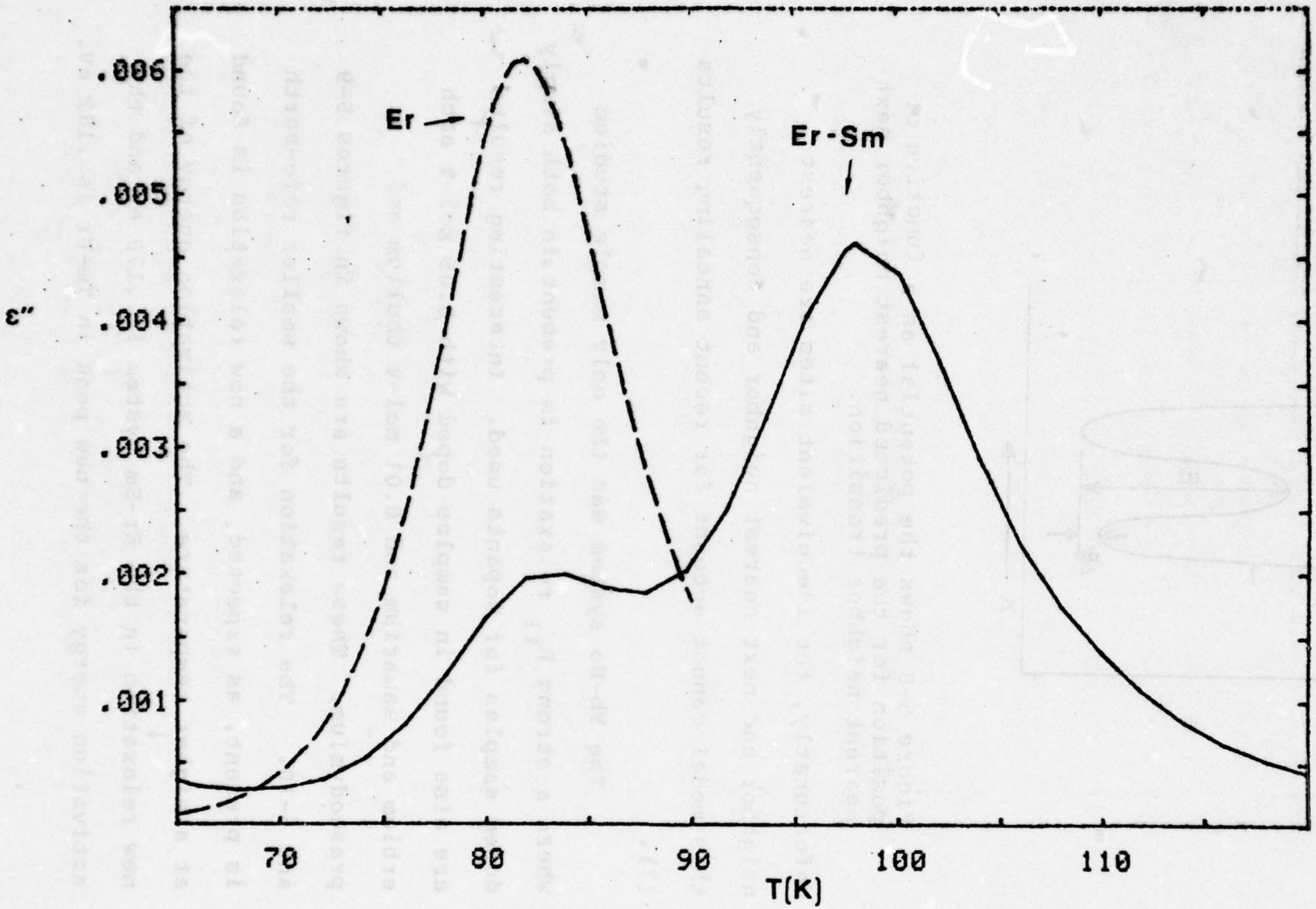


Figure 5-9 shows the results for the Er-Sm sample. A theoretical Er relaxation is also shown.

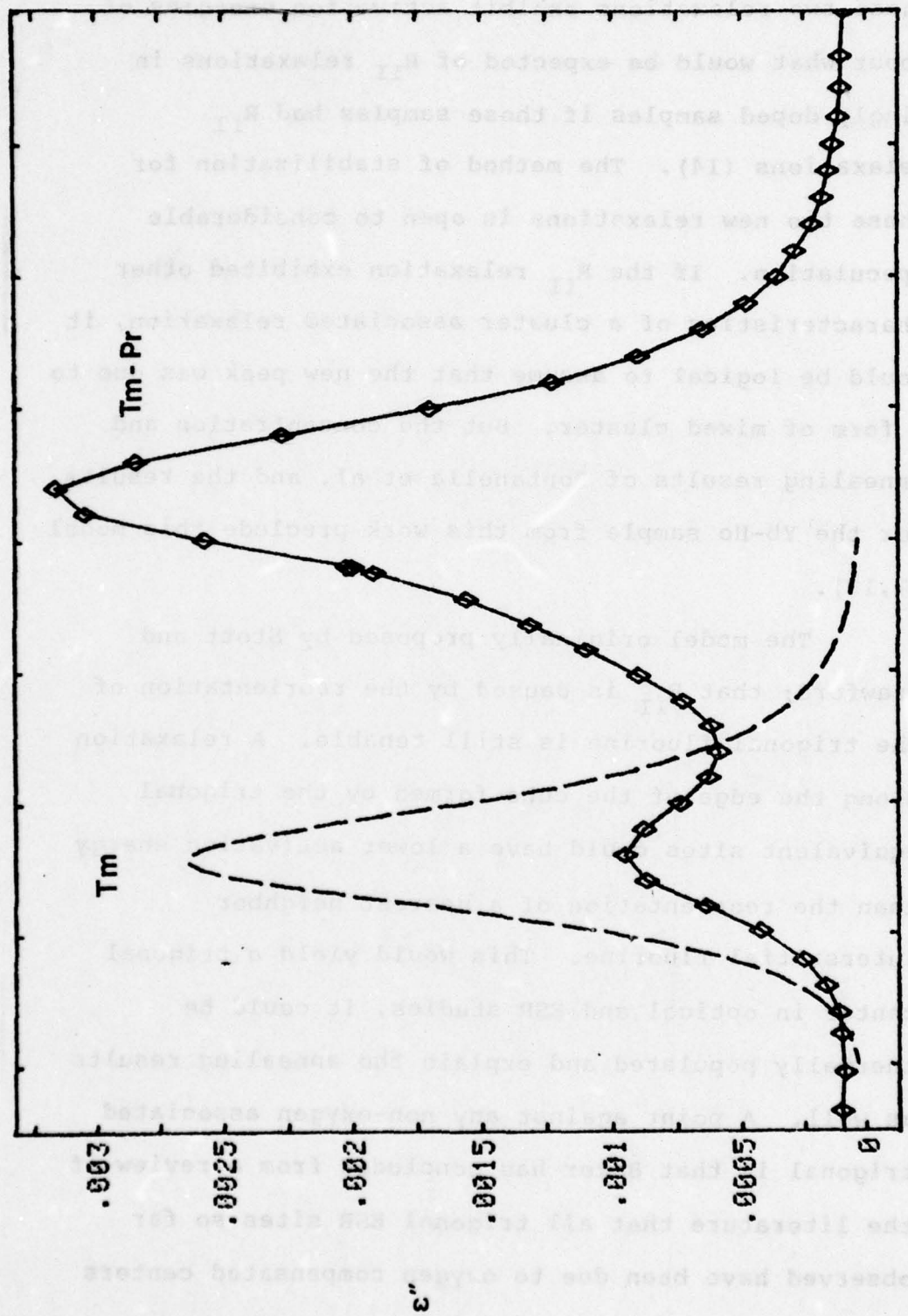


Figure 5-10 shows the results for the Tm-Pr sample. A theoretical Tm relaxation is also shown.

These two relaxations exhibit activation energies of about what would be expected of R_{II} relaxations in singly doped samples if those samples had R_{II} relaxations (14). The method of stabilization for these two new relaxations is open to considerable speculation. If the R_{II} relaxation exhibited other characteristics of a cluster associated relaxation, it would be logical to assume that the new peak was due to a form of mixed cluster. But the concentration and annealing results of Fontanella et al. and the results for the Yb-Ho sample from this work preclude this model (7,13).

The model originally proposed by Stott and Crawford; that R_{II} is caused by the reorientation of the trigonal fluorine is still tenable. A relaxation along the edge of the cube formed by the trigonal equivalent sites could have a lower activation energy than the reorientation of a nearest neighbor interstitial fluorine. This would yield a trigonal center in optical and ESR studies, it could be thermally populated and explain the annealing results as well. A point against any non-oxygen associated trigonal is that Baker has concluded from a review of the literature that all trigonal ESR sites so far observed have been due to oxygen compensated centers

(27). Also, this model fails to explain the non-Arrhenius behavior of the relaxation time. It should be pointed out that most of the ESR work done on rare-earth doped CaF_2 has been done on CaF_2:Gd, and that gadolinium doped CaF_2 has very little or no R_{II} sites at all (14). Also, Varotsos has predicted that all low temperature relaxations should exhibit non-Arrhenius behavior (28).

Figure 5-11 shows the configuration and possible relaxation paths for each of the models. It is not clear whether the charge compensating fluorine moves through the lattice itself or if it moves by replacing a lattice fluorine which then becomes a charge compensator in another site. Both modes have been shown, theoretically, by Catlow to have about the same activation energy. The direct motion of the fluorines is shown.

The R_{III} Relaxation

The R_{III} relaxation is characterized by being the lowest energy, and therefore lowest temperature, relaxation yet observed in rare-earth doped calcium-fluoride (14). It is also known to be a very non-Debye like relaxation. Specifically it has a relaxation time that is non-Arrhenius. This causes it to be

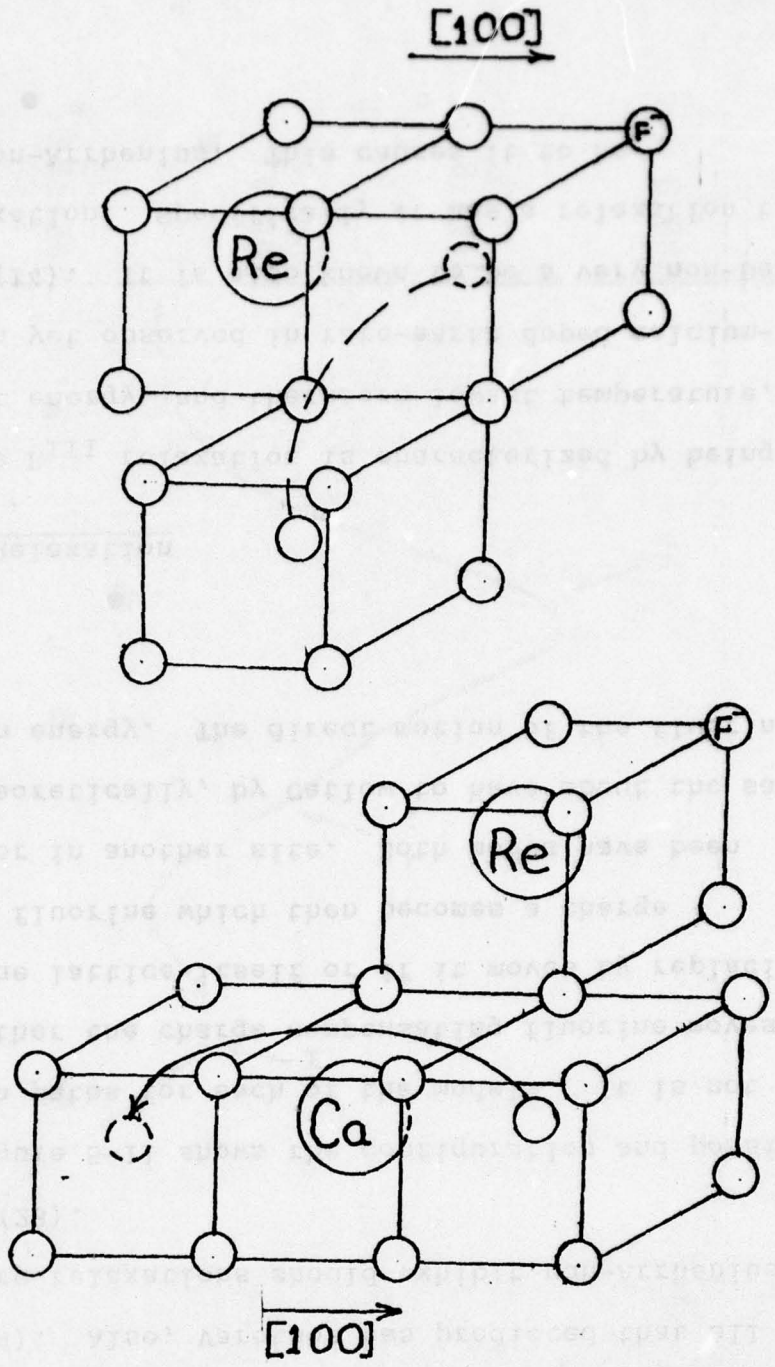


Figure 5-11 shows the two models discussed in the text. The top drawing is the inequivalent site model proposed by Catlow. The bottom drawing shows one possible relaxation mode for the next nearest neighbor interstitial.

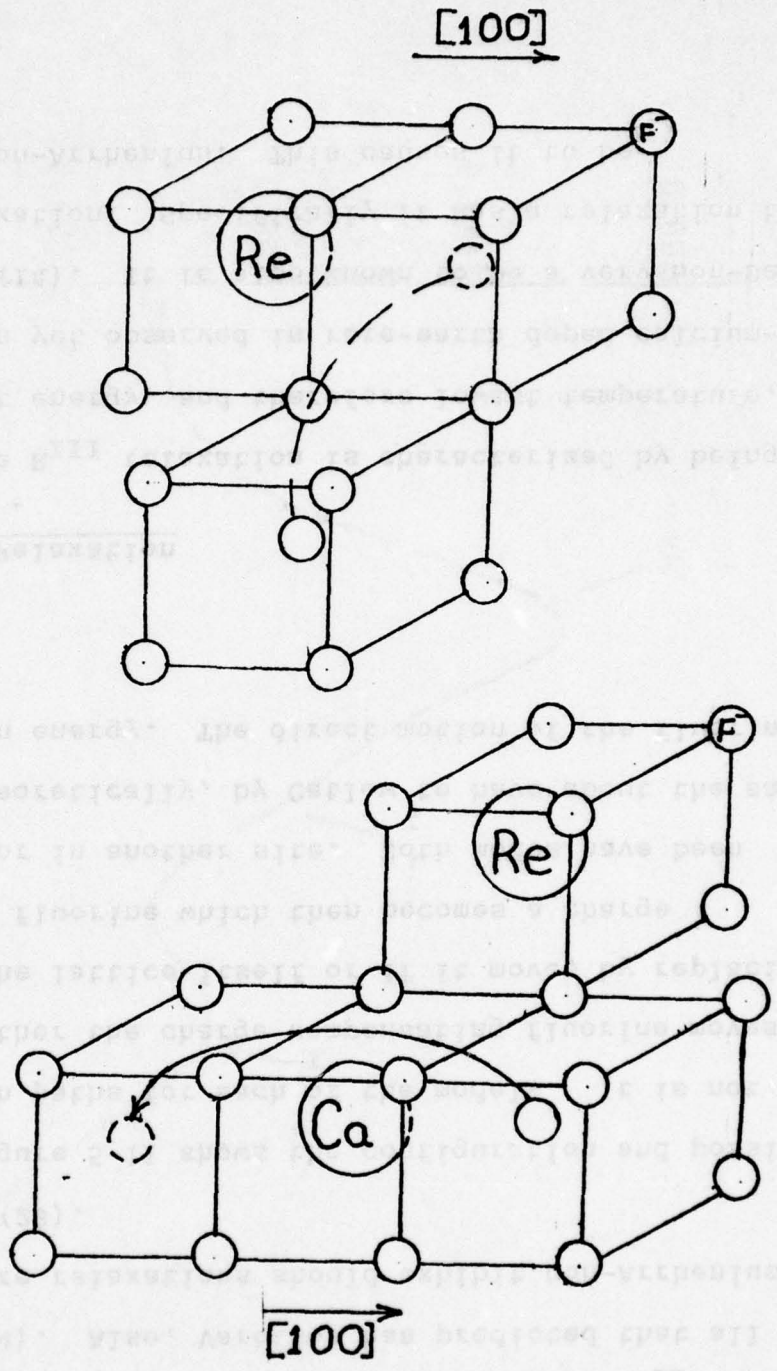


Figure 5-11 shows the two models discussed in the text. The top drawing is the inequivalent site model proposed by Catlow. The bottom drawing shows one possible relaxation mode for the next nearest neighbor interstitial.

significantly broader, and confounds efforts to fit the data for relaxation parameters. When compared with relaxations that have higher activation energies it seems likely that a different relaxation mechanism may be involved. Quantum mechanical tunneling is but one of the possibilities. It also seems likely that the charge carrier that is relaxing is not the same as for the other relaxations since it has such a low activation energy. Instead of a fluorine ion, an electron or some type of hole center may be relaxing.

The strong dependence of the R_{III} on the dopant concentration suggests that the relaxation is some form of cluster associated relaxation (13). Fontanella et al. have suggested that the cluster is of higher order than dimer on the basis of annealing and optical studies. He further goes on to suggest that the site might possibly contain three rare-earths (7).

The most important results of this work again come from the Yb-Ho sample. As can be seen from figure 5-12, the R_{III} relaxations for both of the dopants are present. It does appear, in this 100 Hz plot, that at least one additional relaxation is present in the upper wing of the ytterbium relaxation. This suggests that, as expected, clustering is the source of the R_{III} relaxation.

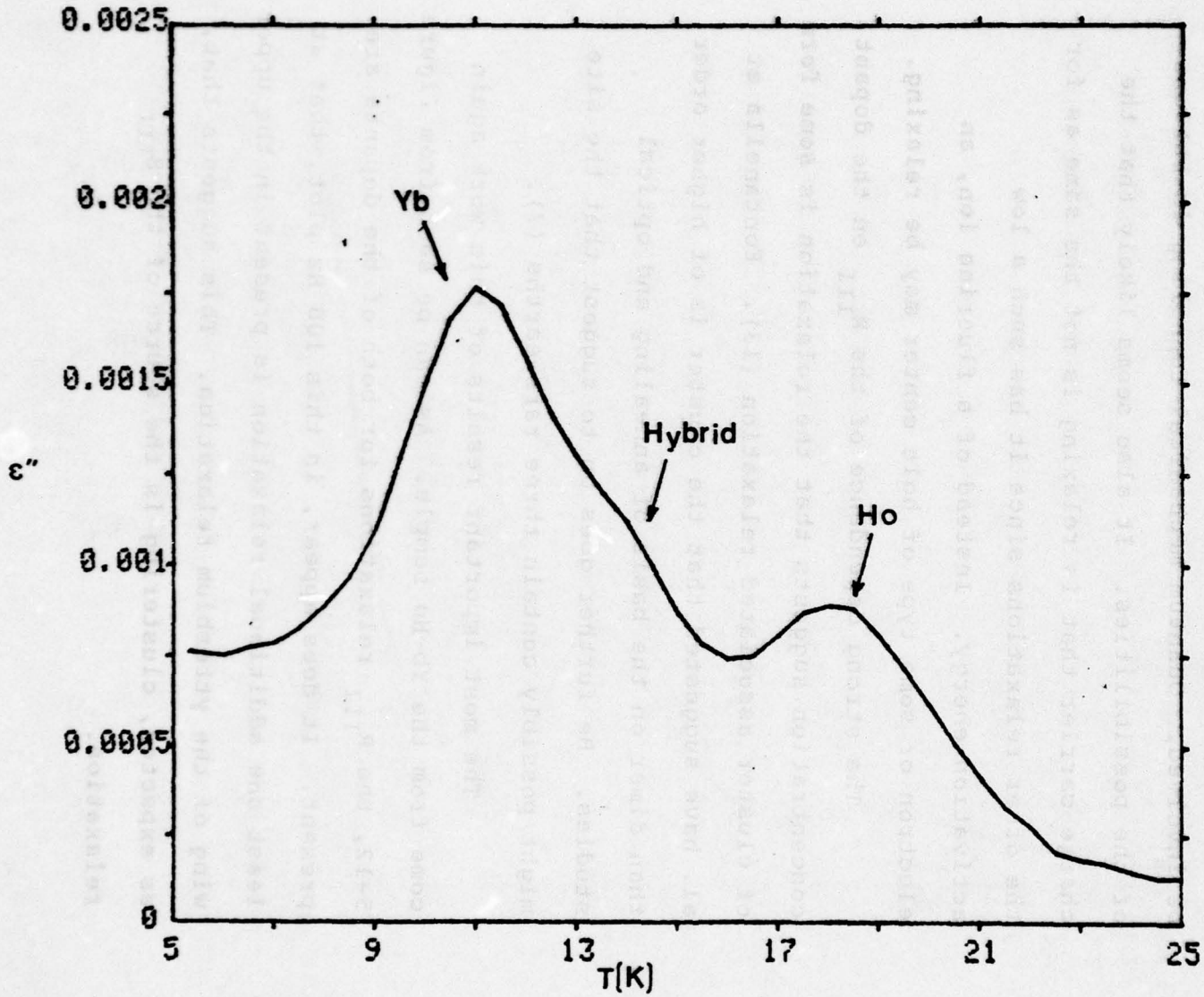


Figure 5-12 shows the relaxations present in the extreme low temperature region for the Yb-Ho sample.

If the R_{III} relaxation is due to a trimer cluster it would be expected to observe four relaxations in a doubly doped sample. One for each pure dopant and one for each two of one type plus one of the other. If the combination were purely random, the two mixed relaxations would be larger by about a factor of three. The tendency of the R_{III} relaxation to favor smaller rare-earths would skew this distribution (14).

There is also a possibility that the R_{III} relaxation may be due to a dimer site since only one new relaxation is observed in the 0.3 mol-% Tb-Tm sample. (figure 5-13) However, the trimer identification is more appealing on the basis of optical absorption studies and the concentration dependence of this relaxation (7,9,13).

The results for the 0.05 mol-% Er-Sm sample are of interest since a new relaxation is clearly seen in the upper wing of the erbium relaxation. No other peaks are present. Samarium exhibits no R_{III} relaxation so it seems possible that the new relaxation is a site involving two erbium ions and one samarium. The Er-Sm relaxations are shown in figure 5-14.

The interpretation of any results in the R_{III} region are questionable at best. At the present time

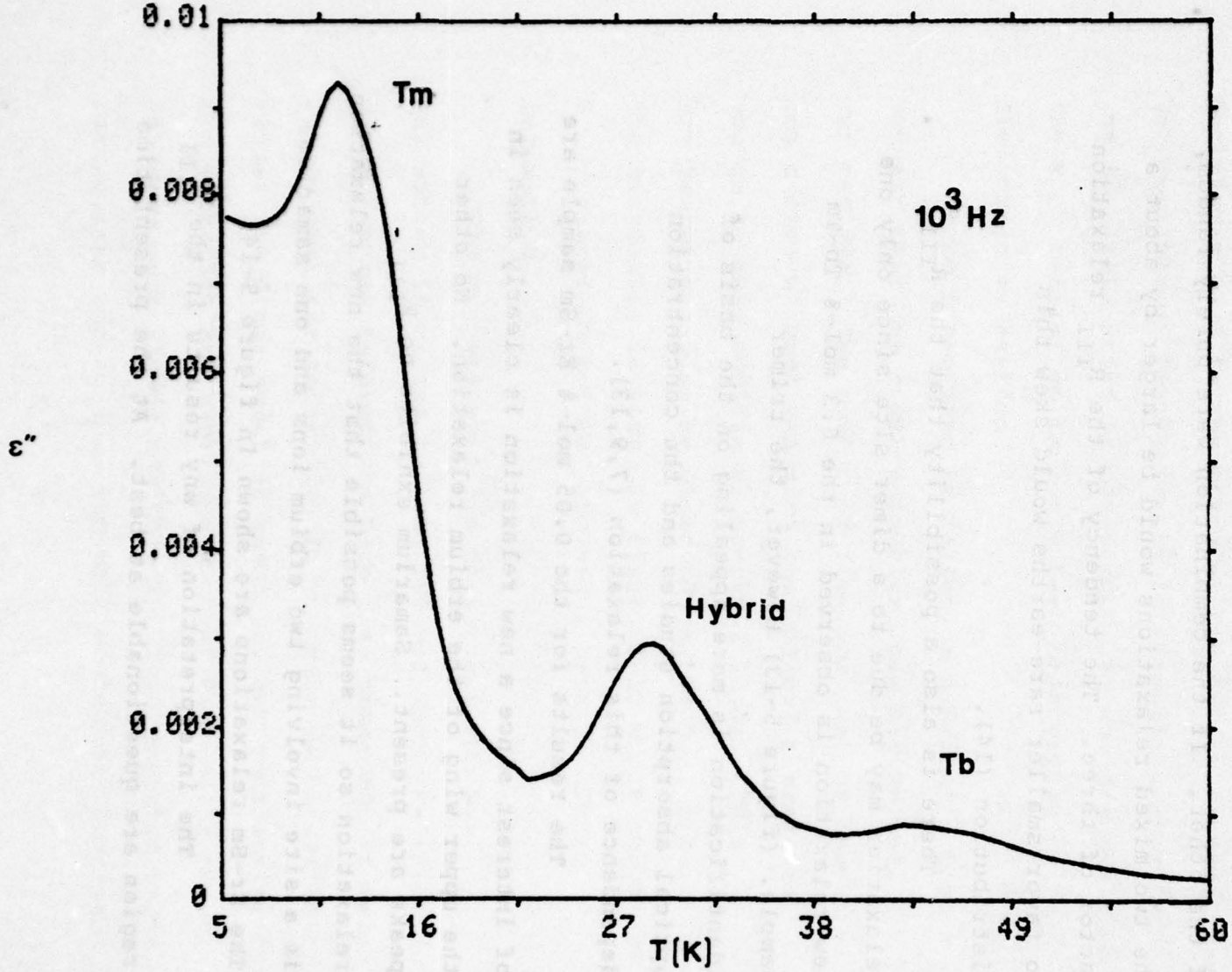


Figure 5-13 shows the relaxations in the Tb-Tm sample. The Tb relaxation is also very small in the singly doped crystals (14).

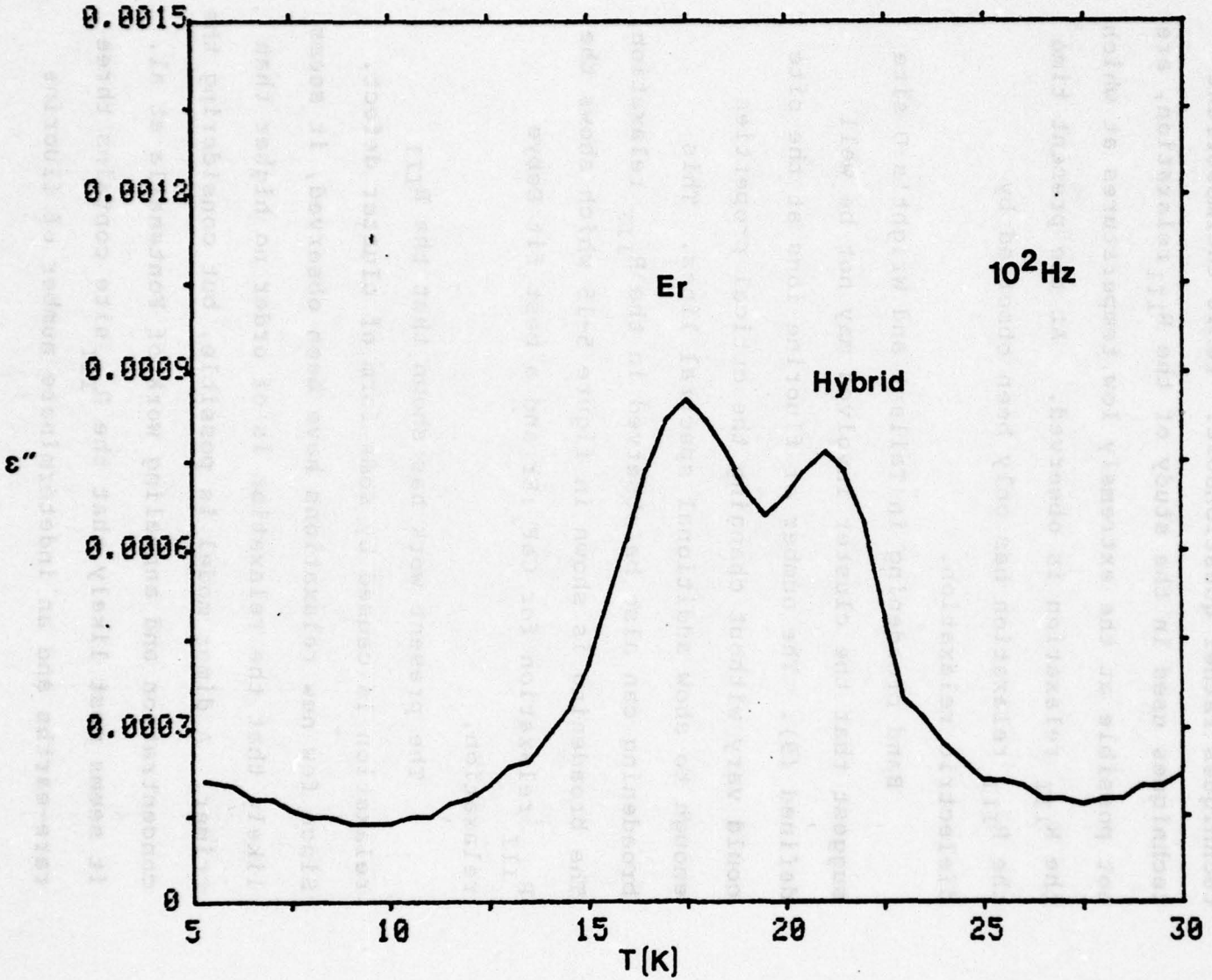


Figure 5-14 shows the results for the Er-Sm sample.

no equation exists to properly describe the R_{III} relaxation process. This makes the use of fitting techniques rather questionable. Ionic thermocurrent techniques used in the study of the R_{III} relaxation, are not possible at the extremely low temperatures at which the R_{III} relaxation is observed. At the present time the R_{III} relaxation has only been observed by dielectric relaxation.

Band broadening in Tallant and Wright's D site suggest that the cluster involved may not be well defined (9). The number of fluorine ions at the site could vary without changing the optical properties enough to show additional spectral lines. This broadening can also be observed in the R_{III} relaxation. The broadening is shown in figure 5-15 which shows the R_{III} relaxation for CaF_2:Er and a best fit Debye relaxation.

The present work has shown that the R_{III} relaxation is caused by some form of cluster defect. Since few new relaxations have been observed, it seems likely that the relaxation is of order no higher than trimer. A dimer model is possible, but considering the concentration and annealing work of Fontanella et al. it seems most likely that the R_{III} site contains three rare-earths and an indeterminate number of fluorine

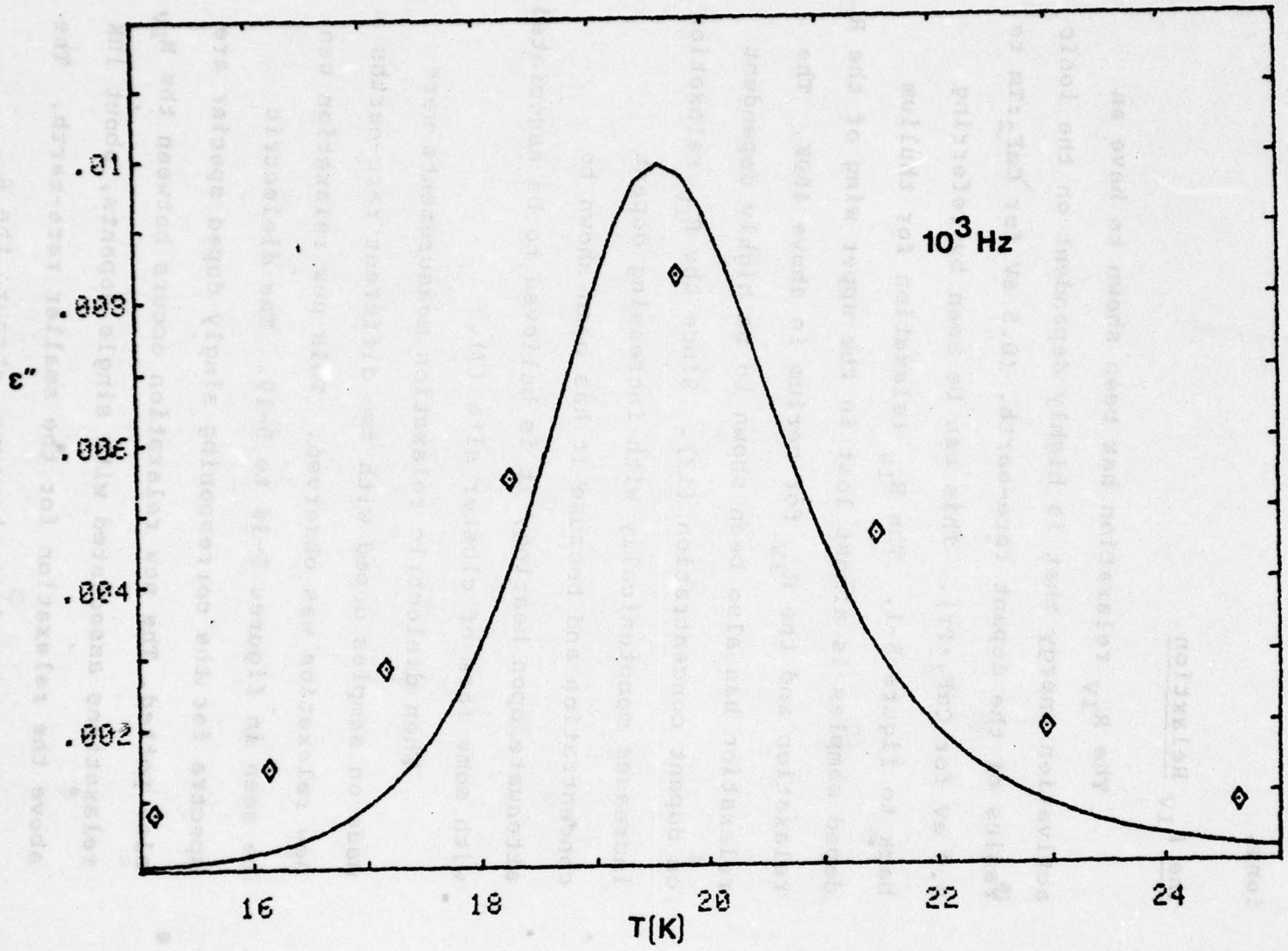


Figure 5-15 shows the broadening of the R_{III} relaxation in an Er doped sample.

ions.

The R_{IV} Relaxtion

The R_{IV} relaxation has been shown to have an activation energy that is highly dependent on the ionic radius of the dopant rare-earth. (0.5 eV for CaF_2:Tm to 0.9 eV for CaF_2:Pr). This can be seen by referring back to figure 5-1. The R_{IV} relaxation for thulium doped samples is almost lost in the upper wing of the R_{IV} relaxation and the R_{IV} for cerium is above 400K. The relaxation has also been shown to be highly dependent on dopant concentration (13). Since the R_{IV} relaxation increases monotonically with increasing dopant concentration and because it has been shown to attenuate upon heating, it is believed to be associated with some form of cluster site (7).

When dielectric relaxation measurements were made on samples doped with two different rare-earths a new relaxation was observed. This new relaxation can be seen in figures 5-16 to 5-19. The dielectric spectra for the corresponing singly doped species are also potted. The new relaxation occurs between the R_{IV} relaxations associated with single dopants, about 10K above the relaxation for the smaller rare-earth. The new relaxation does, however, obscure the R_{IV}

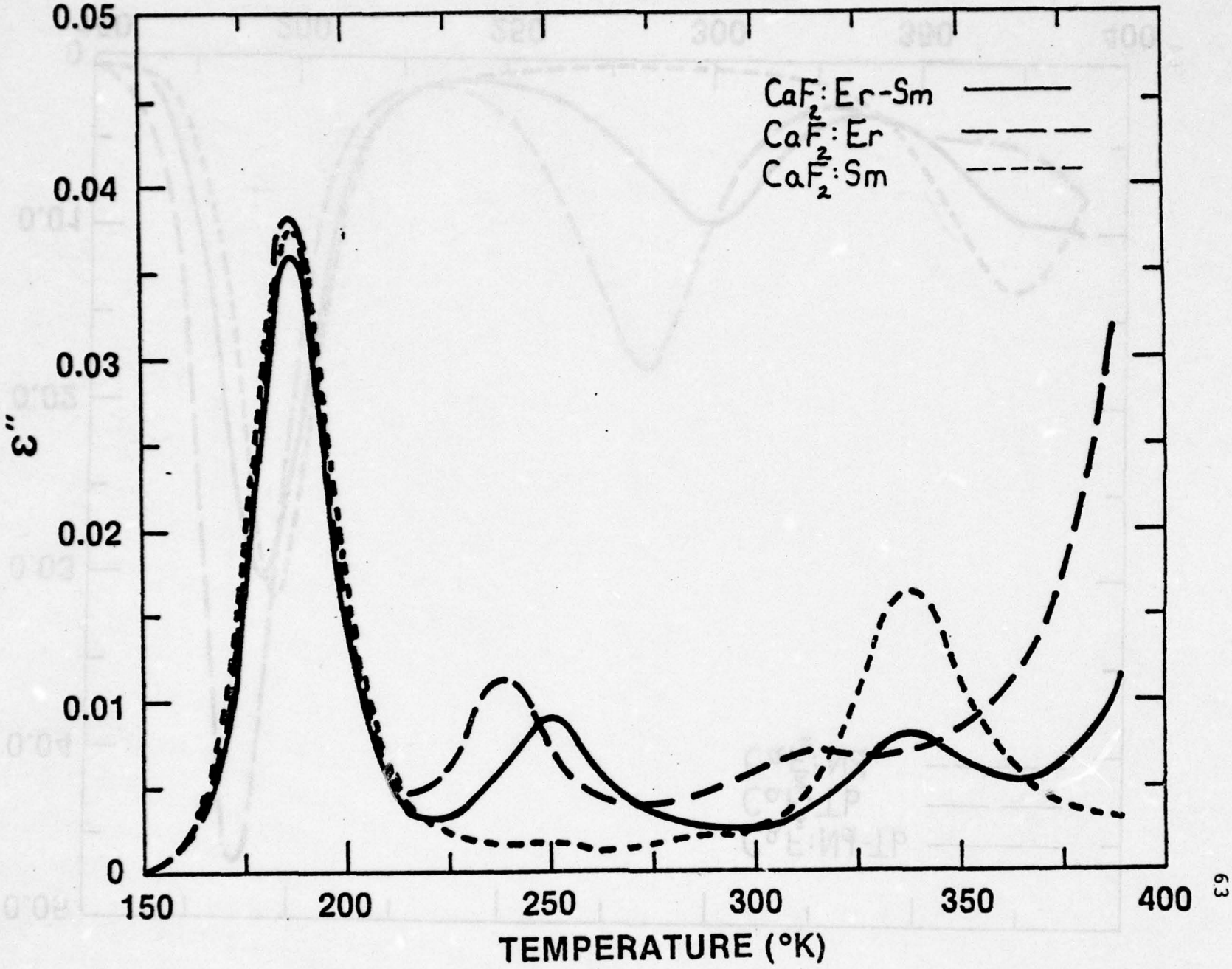


Figure 5-16 shows the high temperature results for the Er-Sm sample.

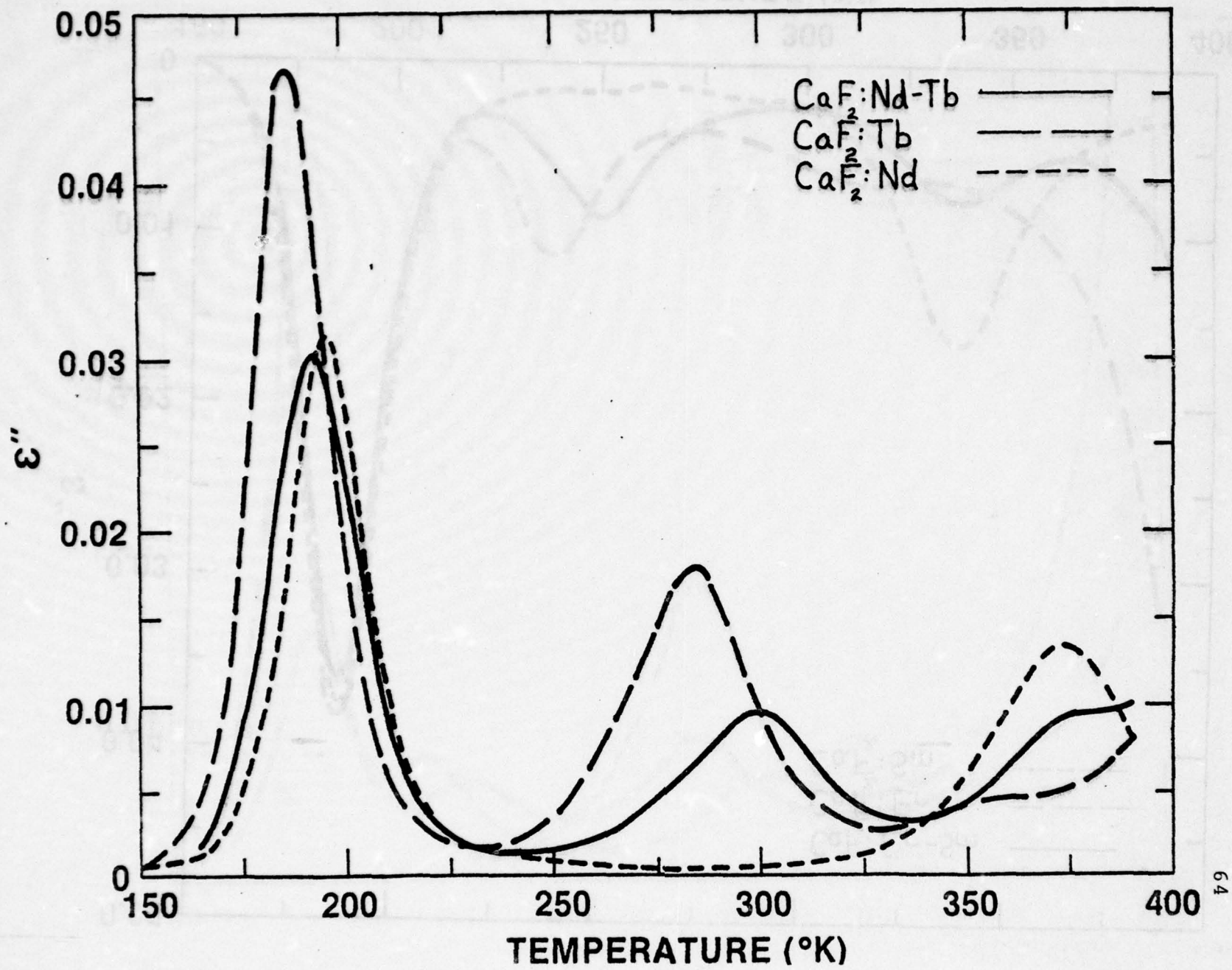


Figure 5-17 shows the high temperature results for the Nd-Tb sample.

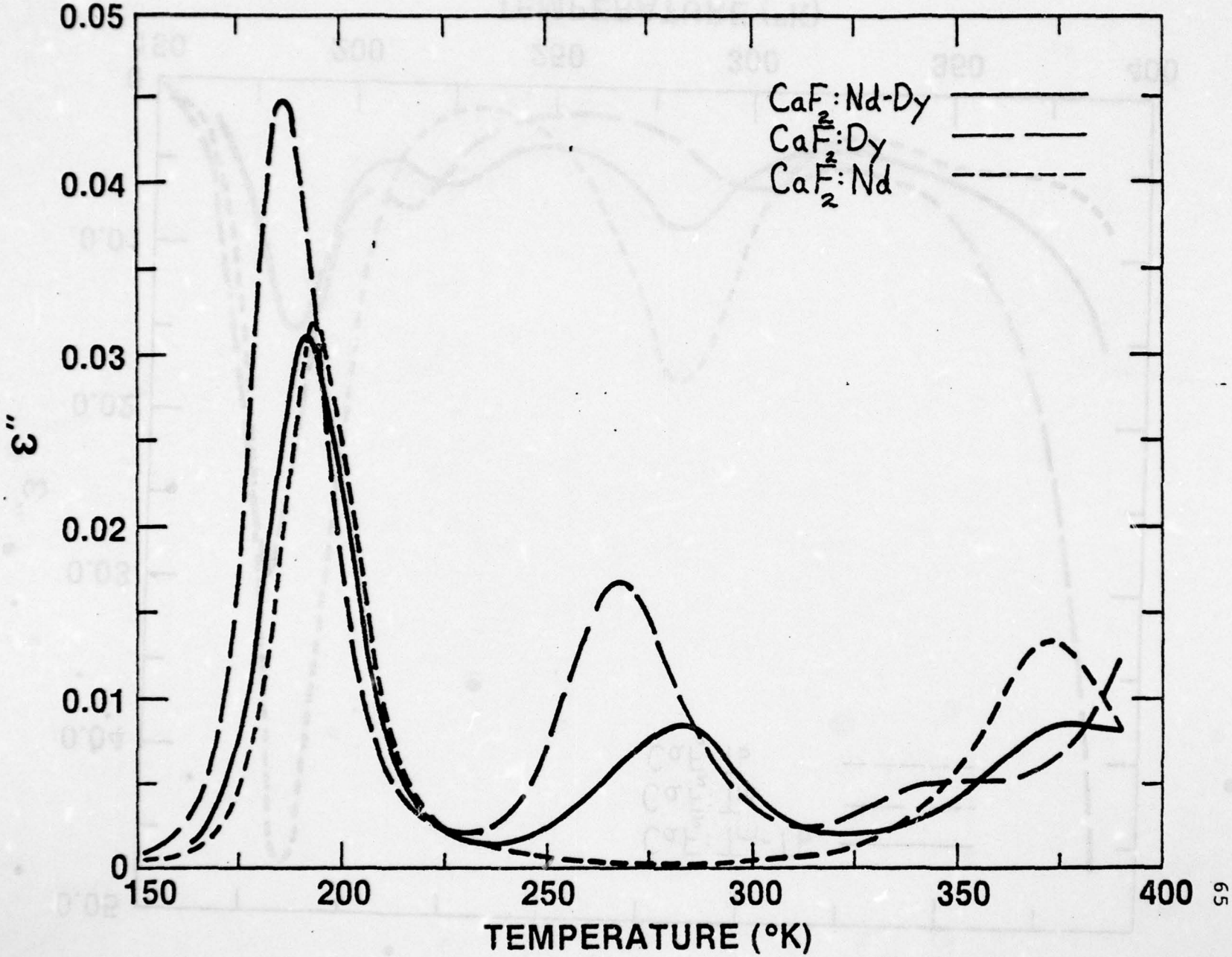


Figure 5-18 shows the high temperature results for the Nd-Dy sample.

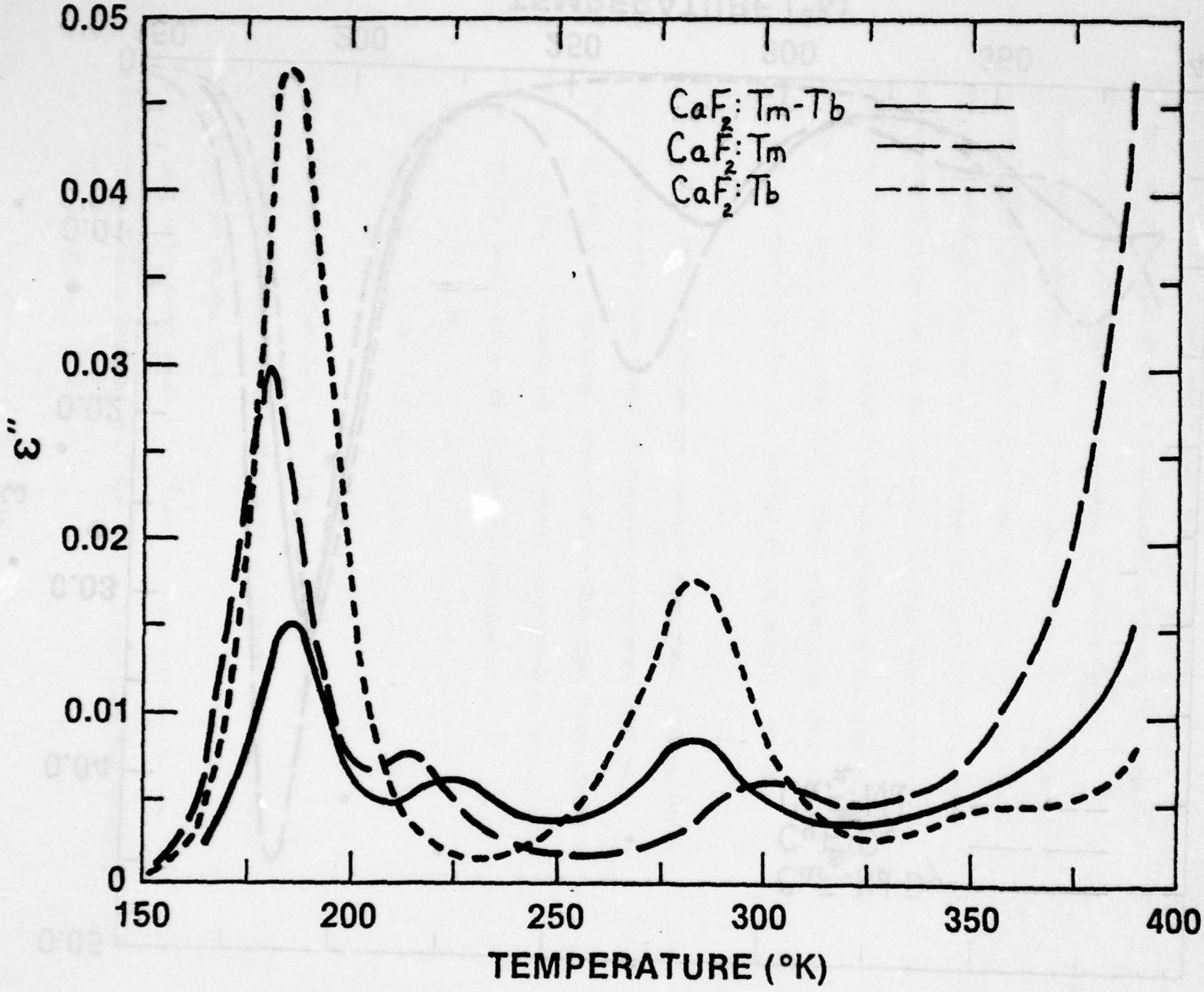


Figure 5-19 shows the high temperature results for the Tm-Tb sample.

relaxation of the smaller rare-earth.

Since the R_{IV} relaxation is not a perfect Debye peak; it is broader than predicted by theory, extensive curve fitting techniques would not provide conclusive proof that the R_{IV} relaxation for the smaller rare-earth is present. To verify the existence of the R_{IV} relaxation for the smaller rare-earth in the lower temperature wing of the new relaxation, ITC peak cleaning methods were employed.

As mentioned earlier, the ITC technique involves the polarization of permanent dipolar structures at a temperature for which the relaxation time of the dipole is very short. If two relaxations are close together in a dielectric relaxation or ITC spectrum they may be separated by selective polarization. This is known as peak cleaning.

In this work, ionic thermocurrent peak cleaning techniques were used to probe for the R_{IV} relaxation for the smaller rare-earth. This measurement was particularly easy since the activation parameters for the single dopant relaxation may be found in the literature (14). The samples were polarized at a temperature where the relaxation time for the smaller rare-earth would be one minute. The samples were polarized for a minute and then cooled. The

polarization of the small rare-earth R_{IV} relaxation for one relaxation time would, by equation 2-9, cause it to be polarized to 63% of the saturation polarization. The new peak, on the other hand, would only be polarized to about 10%. When the sample was heated and the depolarization current measured, the R_{IV} relaxation for the smaller dopant was found. These results are shown in figures 5-20 and 5-21. In the plots the smaller rare-earth relaxation is shown as the same size as the new peak for clarity. The relaxation for the smaller rare-earth is, in fact, about one third the strength.

The activation energies and reciprocal frequency factors for the new relaxations were determined by fitting the peak versus temperature for the temperature where $\omega\tau=1$, for each of the five frequencies employed. The results were then fit to the equation:

$$\ell n\tau = E/kT + \ell n\tau_0 \qquad 5\text{-}2$$

The results of this fit for the new peaks and the activation parameters for the single dopant relaxations are given in table 5-1.

An important point is that in all cases the new relaxation falls just above the R_{IV} relaxation for the

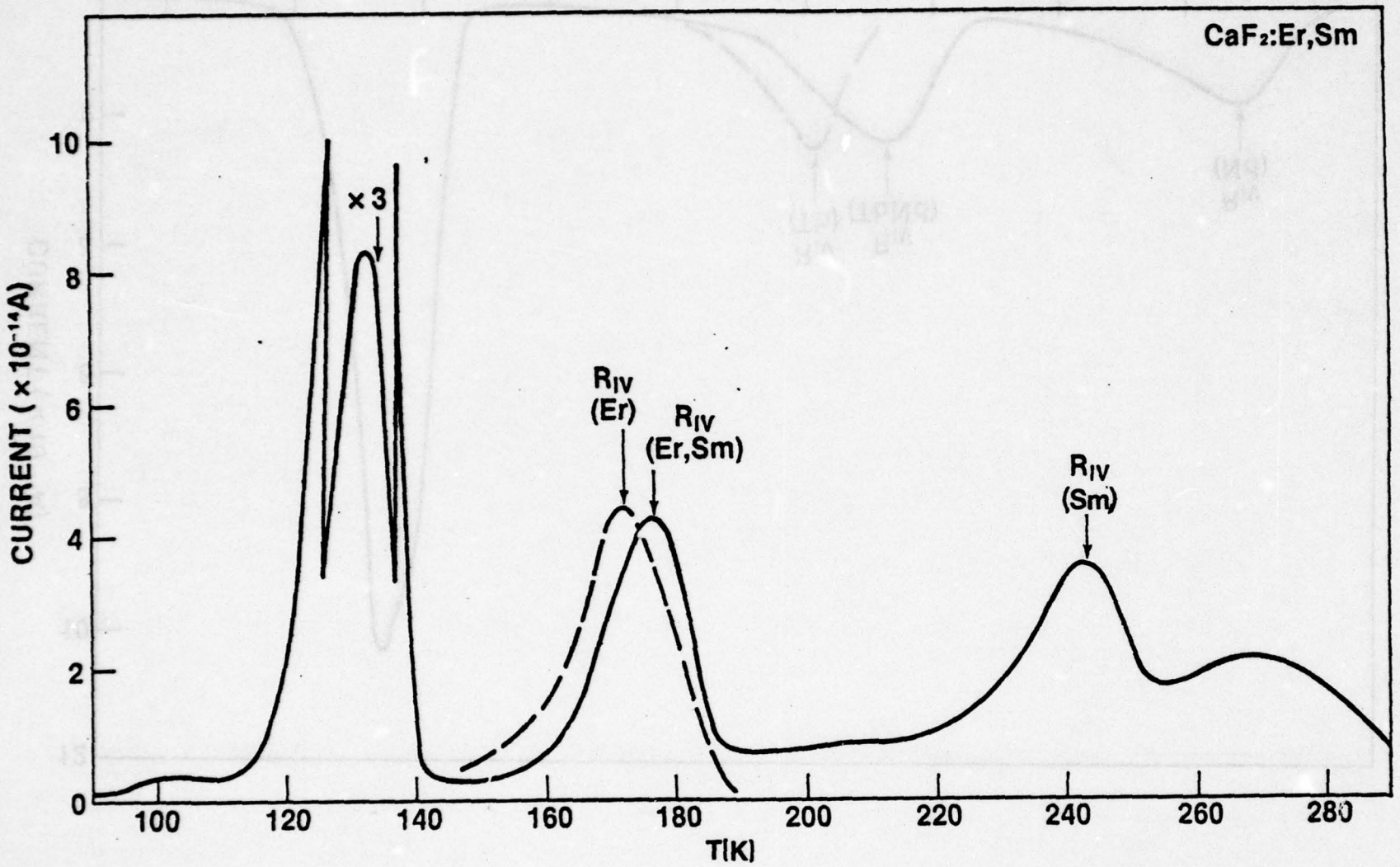


Figure 5-20 shows the ITC results for the Er-Sm sample.

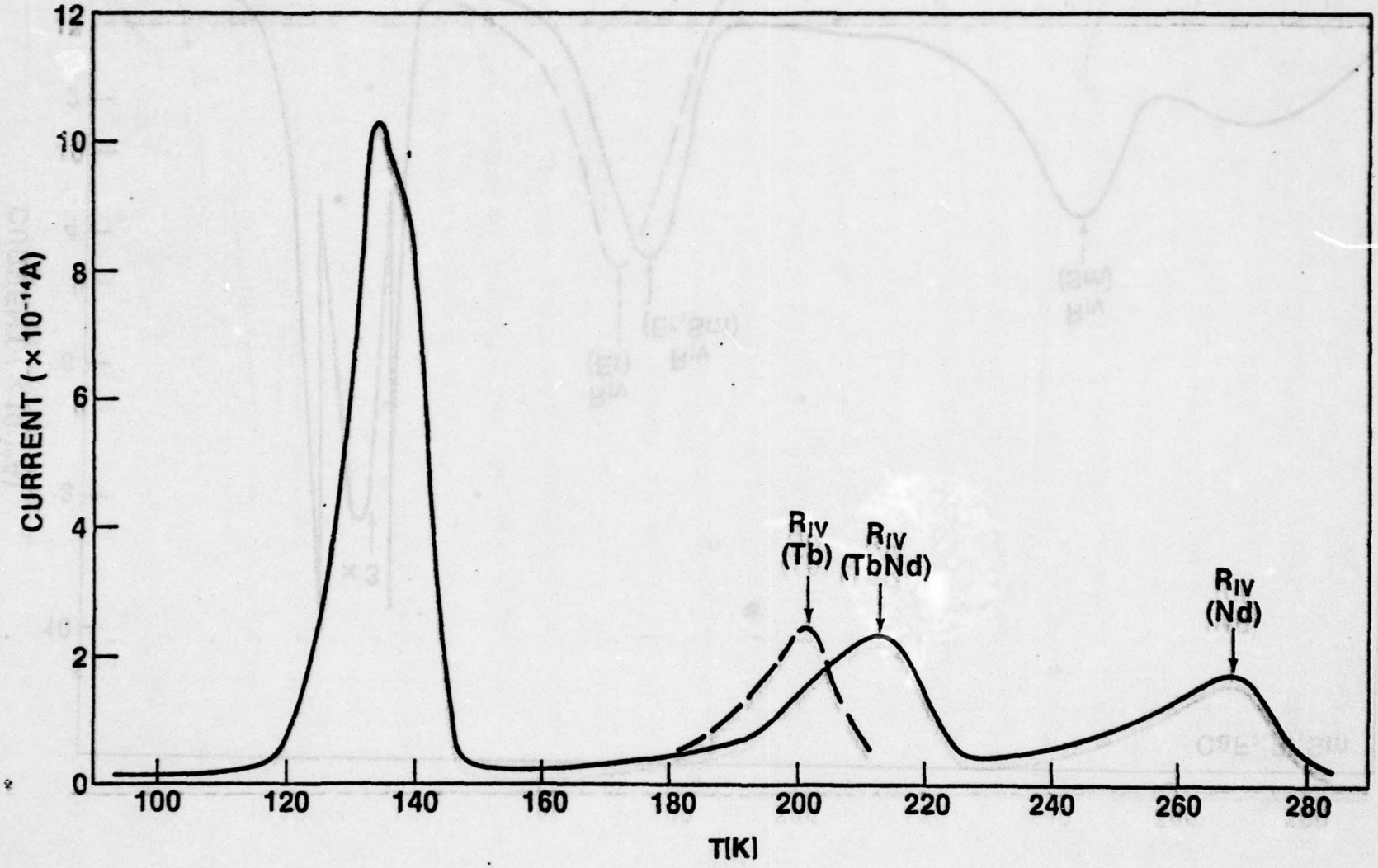


Figure 5-21 shows the ITC results for the Nd-Tb sample.

TABLE 5-1 Activation parameters for the R_{IV} and associated mixed cluster relaxations in rare-earth doped CaF_2. The estimated error in E and $\ell n \tau_0$ is about 1%.

Dopant	E(ev)	$\tau_0(10^{-15}s)$
0.1% Er[a]	0.543	5.51
0.05% Er - 0.05% Sm	0.558	9.11
0.1% Sm[a]	0.793	2.47
0.1% Dy[a]	0.604	7.64
0.05% Dy - 0.05% Nd	0.631	9.04
0.1% Nd[a]	0.89	
0.1% Tb[a]	0.645	5.35
0.05% Tb - 0.05% Nd	0.671	7.86
0.1% Nd[a]	0.89	
0.1% Tm	0.463	26
0.3% Tm - 0.3% Tb	0.478	30
0.3% Tm - 0.3% Tb	0.638	7.2
0.1% Tb[a]	0.645	5.4

a. Reference 14

smaller rare-earth. Of further note is that terbium (Tb) was studied both as the larger rare-earth and as the smaller rare-earth (Tb-Tm and Nd-Tb). In both cases the new relaxation occurs near the smaller dopant.

Since a new relaxation is observed in the region of the R_{IV} for singly doped crystals, it is reasonable to conclude that the new relaxation is some form of hybrid cluster associated relaxation. That is to say; the new relaxation is caused by a defect site that contains at least one of each of the two dopants. Since only one new relaxation is seen it is likely that the new relaxation is a cluster involving one each of the two dopants. Thus the R_{IV} relaxation appears to be due to some type of cluster defect involving two rare-earths, a dimer.

Several dimer models have been proposed in the literature. Many of these do not possess electric dipole moments and would not be expected to relax electrically (5,29). This work does not rule out the existence of these types of defect sites. Evidence exists in the literature that there is , in fact, more than one type of dimer defect in rare-earth doped calcium fluoride (9).

The results of this work may be explained by

several models. One of these was proposed by Yaney et al. to explain optical data in rare-earth doped strontium fluoride (30). In this model, a neutral dimer is formed by two rare-earths in a nearest neighbor configuration along the [110] axis, with charge compensating fluorine ions occupying nearest neighbor sites along the [110] axis. This dimer has no dipole moment. But if an additional fluorine ion were to be attracted or "gettered" to this site it could be expected to relax around either of the rare-earths. While this defect model seems unlikely, from an electro-static standpoint, it explains the "anomalous" increase in non-locally compensated cubic sites that has been observed with increasing dopant concentration (31-33).

Another type of non-neutrally charged defect, that has been proposed by Andeen et al., again involves two rare-earths occupying [110] nearest neighbor sites and a fluorine ion relaxing between them in the [110] direction (14). It, like the gettering model, is electro-statically unfavorable. In its favor, this model explains the strong dependence of the R_{IV} on dopant ionic radius.

A model that would explain the strong association between the position of the hybrid R_{IV}

relaxation and the smaller rare-earth would be two rare-earths occupying sites along the [100] direction with a fluorine between them. A second fluorine ion could relax around either of the rare-earths. This model is attractive since it is electrically neutral and can be used to explain the dependence of the hybrid relaxation on the smaller rare-earth. However, it has been suggested by Tallant and Wright that their C site has approximate trigonal symmetry (34). A slight modification of the above model would place the two rare-earths along the [111] axis with a fluorine ion between them in a next nearest neighbor site and an additional fluorine relaxing about either rare-earth ion would have almost trigonal symmetry. This model would also explain the association between the position of the hybrid relaxation and the smaller dopant. A diagram of each of the models presented is shown in figure 5-22.

The cluster origin of the R_{IV} relaxation has been demonstrated. It is likely that the relaxation is due to a cluster of two rare-earths; a dimer. Also it has been shown that the hybrid relaxation is more dependent on the smaller dopant. This should be important in defining the relaxation mechanism of the R_{IV} relaxation.

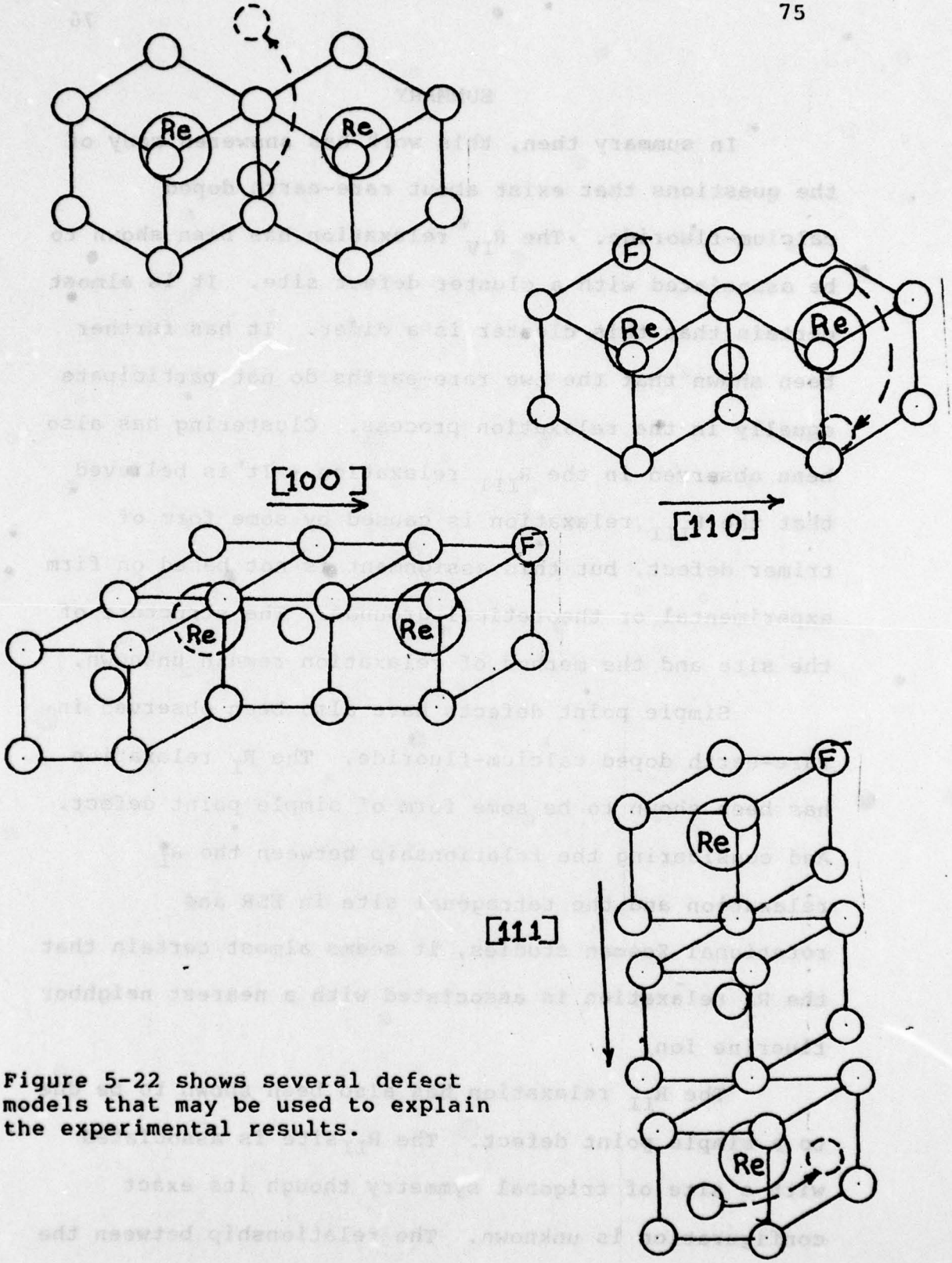


Figure 5-22 shows several defect models that may be used to explain the experimental results.

SUMMARY

In summary then, this work has answered many of the questions that exist about rare-earth doped calcium-fluoride. The R_{IV} relaxation has been shown to be associated with a cluster defect site. It is almost certain that this cluster is a dimer. It has further been shown that the two rare-earths do not participate equally in the relaxation process. Clustering has also been observed in the R_{III} relaxation. It is believed that the R_{III} relaxation is caused by some form of trimer defect, but this assignment is not based on firm experimental or theoretical grounds. The structure of the site and the method of relaxation remain unknown.

Simple point defects have also been observed in rare-earth doped calcium-fluoride. The R_I relaxation has been shown to be some form of simple point defect. And considering the relationship between the R_I relaxation and the tetragonal site in ESR and rotational Zeeman studies, it seems almost certain that the R_I relaxation is associated with a nearest neighbor fluorine ion.

The R_{II} relaxation has also been shown to be due to a simple point defect. The R_{II} site is associated with a site of trigonal symmetry though its exact configuration is unknown. The relationship between the

R_{II} relaxation and a next nearest neighbor charge compensation scheme could be argued. But it seems insufficient to explain annealing results.

Several avenues of research should be pursued in order to more fully understand the defect structure of rare-earth doped calcium-fluoride. An improved theoretical model for low energy relaxations should be developed to more fully understand the R_{III} and R_{II} relaxations. Optical absorption and ESR work on doubly doped samples could also prove useful. A greater theoretical understanding of non-Debye like behavior in cluster associated relaxations might yield insight into the configuration of the defect causing the R_{IV} relaxation.

Prior to this work, great strides had been made towards understanding the defect structure of rare-earth doped CaF_2. The results of this work have expanded this body of knowledge to a point where a comprehensive model of this system may be expected soon.

References

1. M.J. Weber and R.W. Bierig, Phys Rev. 134, A1492 (1964).

2. C. Yang, S. Lee, and A.J. Bevolo, Phys. Rev. B13, 2762 (1976).

3. A. Edgar and H.K. Welsh, J. Phys. C: Solid State Phys. 4, L336 (1975).

4. A.D. Franklin and J. Crissman, J. Phys. C: Solid State Phys. 84, L239 (1971)

5. R.J. Booth, M.R. Mustafa, and B.R. McGarvey, Phys. Rev. B17, 4150 (1978).

6. M.R. Mustafa, W.E. Jones, B.R. McGarvey, J. Chem. Phys. 62, 2700 (1975).

7. J.J. Fontanella, D.J. Treacy, and C.G. Andeen, Submitted to J. Chem. Phys.

8. J.B. Fenn, Jr., J.C. Wright, and F.K. Fong, J. Chem. Phys. 59, 5591 (1973).

9. D.R. Tallant and J.C. Wright, J. Chem. Phys. 63, 2974 (1975).

10. B.S.H. Royce and S. Mascarenhas, Phys. Rev. Lett. 24,98 (1970).

11. R. Capalletti, E. Okuno, G.E. Matthews, and J.H. Crawford, Jr., Phys. Stat. Sol. (a) 47, 619 (1975).

12. C. Borely, F. Gonzalez-Jimenez, P. Imbert, and F. Varret, J. Phys. Chem. Solids, 36, 683 (1975).

13. J. Fontanella and C. Andeen, J. Phys. C: Solid State Phys. 9, 1055 (1976).

14. C. Andeen, D. Link, and J. Fontanella, Phys. Rev. B16, 3762 (1977).

15. C.R.A. Catlow, J. Phys. C: Solid State Phys. 6, 64 (1973); J. Phys C: Solid State Phys. 9, 1859 (1976).

16. S.L. Naberhuis and F.K. Fong, J. Chem. Phys 56, 1174 (1972).

17. J.P. Stott and J.H. Crawford, Jr., Phys. Rev. B4, 668 (1971).

18. Dielectric Relaxation, V.V. Daniel (Academic Press, London, 1967).

19. C. Bucci, and R. Fieschi, Phys. Rev. Lett. 12, 16 (1964).

20. C. Bucci, R. Fieschi, and G. Guidi, Phys. Rev. 148, 816 (1966).

21. H.E. Swanson and E. Tatge, Nat. Bur. Stan. Circ. 539, 69 (1953).

22. R.D. Shannon, Acta Cryst. A32, 751 (1976).

23. C.W. Rector, B.C. Pandey, and H.W. Moos, J. Chem. Phys. 45,171 (1966).

24. A.D. Franklin and S. Marzullo, J. Phys. C: Solid State Phys. 3, L171 (1970).

25. E.L. Kitts, Jr., M. Ikeya, and J.H. Crawford, Jr., Phys. Rev. B8, 5840 (1973).

26. G.E. Matthews, Jr. and J.H. Crawford, Jr., Phys. Rev. B15, 55 (1977).

27. Crystals With the Fluorite Structure, edited by W. Hayes (Clarendon, Oxford, 1974).

28. P. Varotsos, (Private Communication).

29. A.K. Cheetham, B.E.F. Fender, and M.J. Cooper, J. Phys. C: Solid State Phys. 4, 3107 (1971).

30. P.P. Yaney, D.M. Schaeffer, and J.L. Wolf, Phys. Rev. B11, 2460 (1975).

31. E. Secemski and W. Low, J. Chem. Phys. 64,4240 (1976).

32. J.M. O'Hare, T.P. Graham, and G.T. Johnston, J. Chem. Phys. 64, 4242 (1976).

33. F.K. Fong, J. Chem. Phys. 64, 4143 (1976).

34. J.R. Tallant and J.C. Wright, J. Chem. Phys. 63, 2074 (1975).

Pre-print to be published in 15 May Physical Review

PB505151 PLRBA,15MAY9BZ1013,3

Electric dipole relaxation of mixed clusters in double-doped CaF_2

Carl Andeen
Physics Department, Case Western Reserve University, Cleveland, Ohio 44106

G. Eric Matthews, Jr.
Naval Research Laboratory, Washington, D.C. 20375

Michael K. Smith and John Fontanella
Physics Department, U.S. Naval Academy, Annapolis, Maryland 21402

(Received 14 December 1978)

Audiofrequency dielectric relaxation measurements from 150 to 400 K and ionic-thermocurrent measurements from 90 to 290 K have been used to study the relaxation of dipolar defects in several calcium-fluoride samples doped with two rare-earth species. In particular, the region containing the R_{IV} relaxation for the corresponding singly doped samples has been investigated. The R_{IV} relaxation is distinguished by an activation energy that is a strong function of the ionic radius of the rare-earth dopant, varying from about 0.5 eV (for CaF_2:Tm) to about 0.9 eV (for CaF_2:Pr). In each doubly doped sample, relaxations are observed similar to those observed in the singly doped samples. In addition, a new relaxation is found which falls between the R_{IV} relaxation peaks of the two constituents. This suggests that the R_{IV} relaxation is associated with a cluster including two rare earths (a dimer) and that the new peak is associated with a cluster including two different rare earths (a mixed dimer). Since the existence of an electrical relaxation requires that the dimer be dipolar, the results cannot be explained by the usual dimer models. In addition, the data indicate that the rare-earth ions do not share equally in the reorientation process.

PACS numbers: 77.40. + i, 61.70.Bv

I. INTRODUCTION

In the past few years, it has become apparent that clustering is significant in rare-earth-doped calcium fluoride at rather low concentrations. Aggregation has, in fact, been observed using dielectric relaxation,[1,2] ionic thermocurrents,[3] selective laser excitation,[4] nuclear magnetic resonance,[5] optical,[6] Mössbauer,[7] neutron diffraction,[8] and electron-spin-resonance[9] techniques. In addition, aggregation has been treated theoretically.[10] Of particular interest here is a center with a relaxation energy of from 0.5 eV (for CaF_2:Tm) to 0.9 eV (for CaF_2:Pr) designated the R_{IV} center by Andeen *et al.*[2] The activation energy was observed to correlate strongly with dopant ion size. There has been evidence that the R_{IV} center is some form of cluster.[2,3,11]

In this paper we report a study of the R_{IV} relaxation region in samples of doubly doped CaF_2 using dielectric relaxation and ionic thermocurrent (ITC) techniques. We have found that, for each system studied, a new relaxation appears between those of the R_{IV} centers associated with each of the constituent dopants providing strong evidence that the R_{IV} relaxation is associated with two rare earths (a dimer). The results are discussed in terms of models for dimers already existing in the literature.

II. EXPERIMENT

Samples of calcium fluoride doped with 0.05 mol% each of erbium and samarium, 0.05 mol% each of neodymium and dysprosium, 0.05 mol% each of neodymium and terbium, and 0.3 mol% each of terbium and thulium were obtained from Optovac, Inc.

Three terminal capacitance C and conductance divided by the frequency G/ω measurements were performed on the samples using a specially modified General Radio 165 bridge. The samples were 25.4-mm-diam disks 1.5-mm thick that had aluminum electrodes evaporated onto their surfaces in the standard three-terminal configuration. The measurements were performed isothermally at five audio frequencies from 10^2 to 10^4 Hz at various temperatures from 150 to 380 K. Further details of the apparatus are given elsewhere.[2]

In the present work, the real part of the dielectric constant ϵ' at 300 K and 1000 Hz was taken to be 6.915 for all samples. ϵ' at 300 K and frequencies other than 1000 Hz was then calculated assuming that the relative change in dielectric constant with frequency is equal to the relative change in capacitance. The real part of the dielectric constant at temperatures other than 300 K for each frequency was then determined from

$$\frac{\epsilon'_T}{\epsilon'_{300}} = \frac{C_T}{C_{300}} \exp\left(-\int_{300}^{T} \alpha_p \, dT\right), \quad (1)$$

where α_p is the isobaric linear thermal expansion coefficient taken to be equal to that for pure calcium fluoride[12] due to a lack of values for rare-earth-doped samples. Finally, the imaginary part of the dielectric constant, ϵ'', was calculated from the equation

$$\epsilon'' = \epsilon' G/\omega C. \quad (2)$$

Ionic-thermocurrent spectra were measured from 90 to 290 K at heating rates of 3–5 K/min. During all ITC experiments the sample chamber was filled with a 1-atm helium exchange gas to minimize thermal gradients. The ITC experiment was performed according to the method developed by Bucci *et al.*[13,14] Polarizing fields of about 8 kV/cm were used, and depolarization currents were measured using a Cary 401 vibrating-reed electrometer. Peak currents were about 10^{-13} A, with a background noise level of about 10^{-15} A. Linear heating rates of 3–5 K/min were employed.

III. RESULTS

The results for the imaginary part of the dielectric constant over the temperature range 150–380 K are plotted in Figs. 1–4 along with previous results for the corresponding singly doped samples.[2]

In Figs. 1–4 the R_{IV} relaxation is the most prominent peak above 200 K for all singly doped samples. In each case the following trend is observed for the doubly doped samples: the expected lower temperature R_{IV} relaxation (small rare earth) is not readily observable in the dielectric loss spectrum, a new relaxation appears at a slightly higher temperature, and the expected higher temperature relaxation (larger rare earth) is observed.

A comparison of the various relaxations is given quantitatively in Table I where activation energies E and reciprocal frequency factors τ_0 are tabulated. The values of E and τ_0 were determined as follows. First, each peak was fitted to the Debye equation for ϵ'':

$$\epsilon'' = (\epsilon'_L - \epsilon'_H)\omega\tau/(1+\omega^2\tau^2), \quad (3)$$

where ϵ'_L and ϵ'_H are the "low"- and "high"-frequency limits of the dielectric constant where "low" and "high" mean relative to the dispersion produced by the relaxation only. τ is the relaxa-

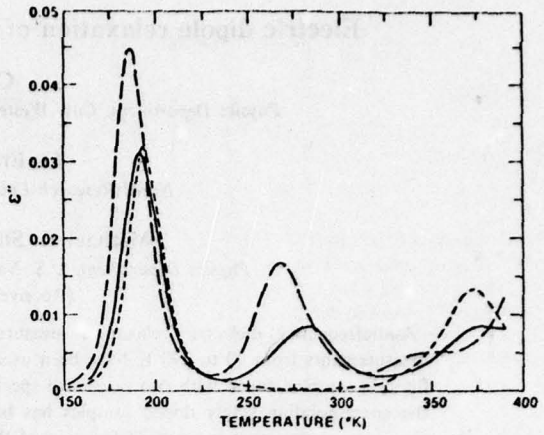


FIG. 2. ϵ'' temperature for various samples of rare-earth-doped calcium fluoride. ———CaF_2:Dy, Nd 0.05 mol % each; — —CaF_2:Dy 0.1 mol %; — — — —CaF_2:Nd 0.1 mol %.

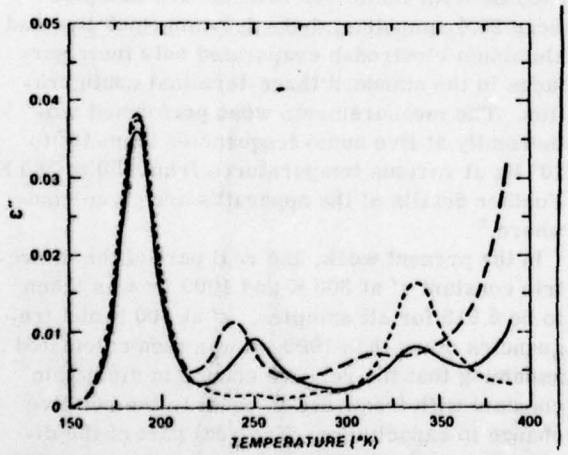


FIG. 1. ϵ'' temperature for various samples of rare-earth-doped calcium fluoride. ———CaF_2:Er, Sm, 0.05 mol % each; — — CaF_2:Er, 0.1 mol %; — — — —CaF_2: Sm, 0.1 mol %.

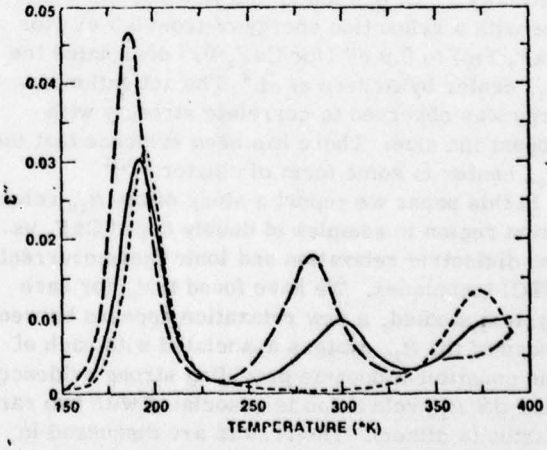


FIG. 3. ϵ'' temperature for various samples of rare-earth-doped calcium fluoride. ———CaF_2:Nd, Tb 0.05 mol % each; — — — —CaF_2:Nd 0.1 mol %; — —CaF_2:Tb 0.1 mol %.

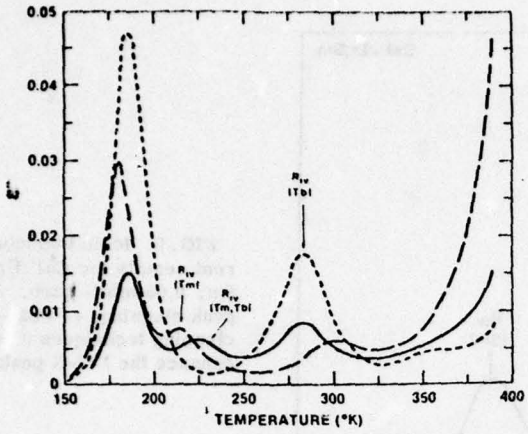


FIG. 4. ϵ'' temperature for various samples of rare-earth-doped calcium fluoride. ———CaF_2:Tm, Tb 0.3 mol% each; — — —CaF_2:Tm 0.1 mol%: — — — —CaF_2: Tb 0.1 mol%.

tion time of the dipole assumed to be given by an Arrhenius equation of the form

$$\tau = \tau_0 e^{E/kT}, \tag{4}$$

where T is the absolute temperature and k is Boltzmann's constant. In addition, it is assumed that

$$\epsilon'_L - \epsilon'_H = A/T \tag{5}$$

where the constant

$$A = Np^2/3\epsilon_0 k \tag{6}$$

is known as the dipole strength, N is the dipole concentration, p is the dipole moment, and ϵ_0 is the permittivity of free space. Fits were made for all five frequencies and the results were used to determine the approximate temperature at which $\omega\tau = 1$ for each of the five frequencies. The activation parameters quoted in Table I were then found from a best fit to the equation

$$\ln(\omega) = -E/kT - \ln(\tau_0). \tag{7}$$

The activation parameters for singly doped CaF_2:Tm were determined in the present paper after subtracting off an estimated contribution due to the R_1 relaxation. Consequently, these values are more uncertain than those for R_{1V} in most of the other materials. However, the values are considered better than the estimate given in Ref. 2 based on the peak position at 100 Hz.

It is seen in Table I that both E and τ_0 for the new relaxation in the doubly doped samples are slightly larger than the corresponding activation parameters for R_{1V} for the smaller rare earth.

TABLE I. Activation parameters for the R_{1V} and associated mixed-cluster relaxations in rare-earth-doped CaF_2. The estimated error in E and $\ln\tau_0$ is about 1%.

Dopant (mol%)	E (eV)	τ_0 (10^{-15} sec)
0.1% Er[a]	0.543	5.51
0.05% Er–0.05% Sm	0.558	9.11
0.1% Sm[a]	0.793	2.47
0.1% Dy[a]	0.604	7.64
0.05% Dy–0.05% Nd	0.631	9.04
0.1% Nd[a]	0.89	
0.1% Tb[a]	0.645	5.35
0.05% Tb–0.05% Nd	0.671	7.86
0.1% Nd[a]	0.89	
0.1% Tm	0.463	26
0.3% Tm–0.3% Tb	0.478	30
0.3% Tm–0.3% Tb	0.638	7.2
0.1% Tb[a]	0.645	5.4

[a] Reference 2.

Because of the interference of dielectric loss due to other relaxations or high temperature dc conductivity, it was only possible to obtain activation parameters for the higher temperature relaxation in the doubly doped samples for the Tm-Tb sample. It is seen that to within experimental error the peak is the same as R_{1V} for the larger rare earth. It is interesting to note that terbium was studied both as the larger (Tb-Tm) and the smaller (Tb-Nd) rare earth.

Since the new relaxation is displaced only slightly in all cases from the position of the R_{1V} relaxation of the smaller rare earth, ITC was used as a probe for the presence in the relaxation spectrum of the peak due to the smaller rare earth in the low-temperature shoulder of the new peak. The ITC experiment is ideally suited to this purpose, since "peak-cleaning" techniques, involving selective polarization and/or depolarization at temperatures in the vicinity of the peak of interest, can greatly reduce the intensity of nearby peaks, while only slightly attenuating the peak of interest. Such measurements were made on the CaF_2:Er, Sm samples, and revealed the presence of the peak associated with the R_{1V} relaxation of Er, the smaller rare-earth, as illustrated in Fig. 5. The ITC data shown as a solid curve were taken without peak-cleaning procedures. The dashed curve was taken on the same sample, but with polarization procedures chosen to enhance the Er-associated R_{1V} relaxation. Similarly, peak cleaning of the new peak in the CaF_2:Tb, Nd sample showed the presence of the Tb R_{1V} relaxation as shown in Fig. 6. In each case, the peak associated with the smaller of the rare earths is about one-third the intensity of the newly observed peak.

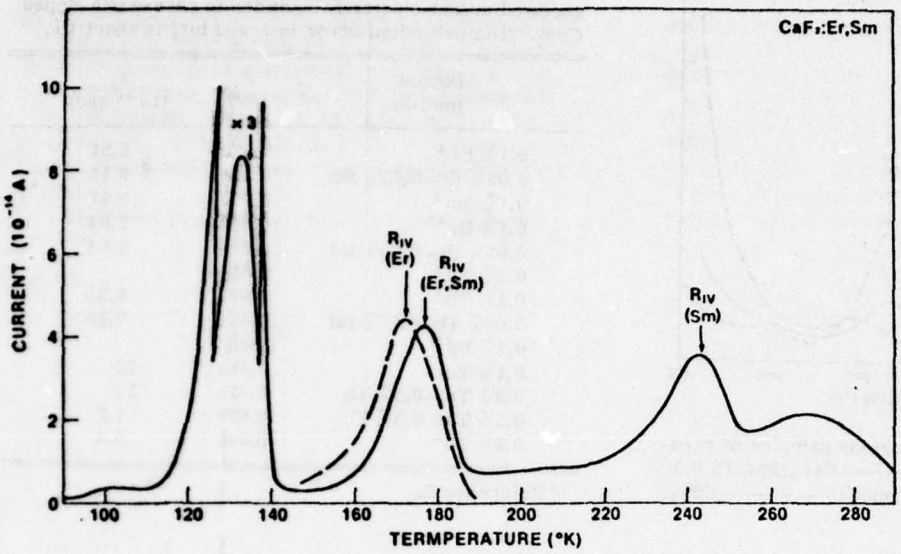


FIG. 5. Ionic thermocurrent results for CaF:Er, Sm, 0.05 mol% each. - No peak cleaning; -- Peak-cleaning techniques used to enhance the 172-K peak.

IV. DISCUSSION

These results strongly suggest that the R_{IV} relaxation is due to a cluster containing more than one rare earth. Furthermore, since only one new peak is observed, it appears likely that only two rare earths are involved in the cluster, the new peak representing a mixed dimer.

Dimers have been observed previously in rare-earth-doped calcium fluoride using techniques other than electrical relaxation. For example, various dimer models have been proposed to explain optical,[6] neutron diffraction,[8] electron-spin-resonance,[9] and selective laser excitation[4] data. However, Booth *et al.*[5] have recently reported dimer-associated nuclear magnetic resonance data that cannot be explained by any dimer models in the literature. The results of the present work also are inconsistent with most of the models in the literature for the following reason. In order for a dimer to relax electrically, it must have a dipole moment. Consequently, neither the dimer with a nearest neighbor pair of rare earths along the [110] direction (see Fig. 1 of Ref. 5, for example) nor the 2-2-2 cluster of Cheetham *et al.*[8] as developed theoretically by Catlow[10] would be

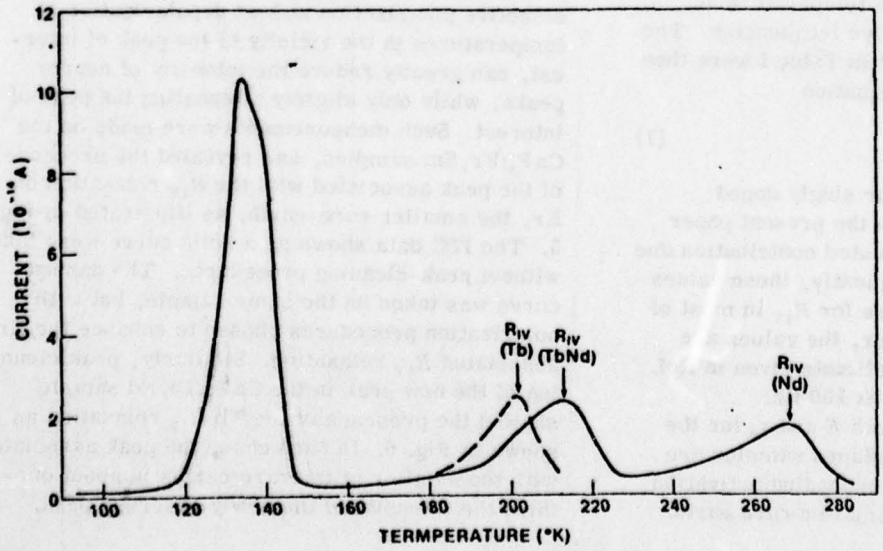


FIG. 6. Ionic thermocurrent results for CaF:Tb,Nd 0.05 mol% each. - No peak cleaning; -- Peak cleaning techniques used to enhance the 202-K peak.

expected to relax electrically. Their existence can't be ruled out on the basis of the present work since they could exist in addition to the dimer reported here. There is, in fact, evidence that more than one type of dimer exists in rare-earth doped calcium fluroide.[4] Furthermore, the dimer reported here may only be a slight modification of those clusters. For example, Andeen *et al.*[2] have speculated that perhaps the dimer is such that the rare earth sits off center. It should be kept in mind that this suggestion was made in an attempt to account for the fact that the activation energy for R_{IV} is strongly dependent upon the size of the rare earth.[2]

It is interesting that the results of the present work are consistent with the "gettering" model of Yaney *et al.*[15] that was proposed to explain optical data in rare-earth-doped strontium fluoride. In that model a dimer extracts an additional interstitial fluoride ion from somewhere in the crystal. If the original dipole were one of the neutral dimers mentioned above, the new dimer would then most likely be endowed with a dipole moment and thus expected to relax electrically. Tallant *et al.*[4] have also found evidence in support of the "gettering" model in rare-earth-doped calcium fluoride. The reason that this model is particularly attractive is that it can be used to explain the "anomalous" increase in cubic sites with increasing rare-earth concentration that is known to exist in CaF_2:Er.[16-18] Specifically, an increase in cubic sites will occur if the dimer extracts its additional interstitial from tetragonal sites.

There are, however, still other ways to form dipolar dimers. For example, either of the "tetragonal" cluster sites proposed by Yaney *et al.*[15] is dipolar though only the monoclinic modification contains equivalent sites necessary for dipolar reorientation. In addition, Andeen *et al.*[2] have speculated on the possible existence of positive dimer ions. While such an entity would seem rather unlikely from an electrostatic point of view, such a cluster has excess rare earths, which is an attractive feature for explaining the strong dependence of E for R_{IV} upon the size of the rare-earth ion.[2]

Finally, the results of the present work show that the dipolar dimer exhibits one other "unusual" feature. It has been shown that the mixed cluster peak does not occur midway between the single specie peaks but is always only slightly shifted in temperature from the position of the peak associated with the smaller rare earth. Consequently, this suggests that the rare earths do not share equally in the reorientation process. This fact should be quite helpful in modeling the reorientation process once the actual structure of the dimer is determined.

V. CONCLUSIONS

In summary, then, it has been shown that in calcium fluoride doped with two different rare earths, a new relaxation is observed in addition to the R_{IV} relaxations observed in singly doped samples. This suggests that the R_{IV} relaxation is associated with a cluster involving two rare earths and that the new relaxation is due to a cluster involving two different rare earths. Since the existence of an electrical relaxation requires that the dimer be dipolar, the results cannot be explained by the usual dimer models. Finally, the data indicate that the rare-earth ions do not share equally in the reorientation process.

ACKNOWLEDGMENTS

The authors would like to thank Donald Schuele of Case Western Reserve University, C. G. Homan of Watervliet Arsenal, Watervliet, New York, and J. R. Miller, III of the U. S. Army Metrology and Calibration Center, Redstone Arsenal, Alabama, for their interest and encouragement. They also acknowledge the helpful administrative and technical assistance of Fred Wasem of the U. S. Naval Academy and thank M. C. Wintersgill and D. Treacy of USNA and B. J. Faraday, N. D. Wilsey, and T. A. Kennedy of the Naval Research Laboratory for many helpful discussions. One of the authors (C. A.) was supported by the U. S. Army Research Office. The remainder of the work was performed under the auspices of the NRL-USNA Cooperative Program for Scientific Exchange.

---

[1] J. Fontanella and C. Andeen, J. Phys. C Phys. 9, 1055 (1976).
[2] C. Andeen, D. Link, and J. Fontanella, Phys. Rev. B 16, 3762 (1977).
[3] R. Capelletti, E. Okuno, G. E. Matthews, and J. H. Crawford, Jr., Phys. Status Solidi A 47, 617 (1978).
[4] D. R. Tallant and J. C. Wright, J. Chem. Phys. 63, 2074 (1975).
[5] R. J. Booth, M. R. Mustafa, and B. R. McGarvey, Phys. Rev. B 17, 4150 (1978); M. R. Mustafa, W. E. Jones, B. R. McGarvey, M. Greenblatt, and E. Banks, J. Chem. Phys. 62, 2700 (1975).
[6] J. B. Fenn, Jr., J. C. Wright, and F. K. Fong, J. Chem. Phys. 59, 5591 (1973).
[7] C. Borely, F. Gonzalez-Jimenez, P. Imbert, and F. Varret, J. Phys. Chem. Solids, 36, 683 (1975).

[8]A. K. Cheetham, B. E. F. Fender, and M. J. Cooper, J. Phys. C 4, 3107 (1971).
[9]N. E. Kask and L. A. Kornienko, Fiz. Tver. Telz. 9, 2291 (1967) [Sov. Phys.-Solid State 9, 1795 (1968)].
[10]C. R. A. Catlow, J. Phys. C, 64 (1973); 9, 1859 (1976).
[11]A. Edgar and H. K. Welsh, J. Phys. C 8, L336 (1975).
[12]A. C. Bailey and B. Yates, Proc. Phys. Soc. 91, 390 (1967).
[13]C. Bucci and R. Fieschi, Phys. Rev. Lett. 12, 16 (1964).
[14]C. Bucci, R. Fieschi, and G. Guidi, Phys. Rev. 148, 816 (1966).
[15]P. P. Yaney, D. M. Schaeffer, and J. L. Wolf, Phys. Rev. B 11, 2460 (1975).
[16]E. Secemski and W. Low, J. Chem. Phys. 64, 4240 (1976).
[17]J. M. O'Hare, T. P. Graham, and G. T. Johnston, J. Chem. Phys. 64, 4242 (1976).
[18]F. K. Fong, J. Chem. Phys. 64, 4143 (1976).

UNCLASSIFIED

SECURITY CLASSIFICATION OF THIS PAGE (When Data Entered)

REPORT DOCUMENTATION PAGE	READ INSTRUCTIONS BEFORE COMPLETING FORM
1. REPORT NUMBER: U.S.N.A. -TSPR; no. 99 (1979)	2. GOVT ACCESSION NO. / 3. RECIPIENT'S CATALOG NUMBER
4. TITLE (and Subtitle): (6) DIPOLAR DEFECTS IN RARE-EARTH DOPED ALKALINE-EARTH FLUORIDES.	5. TYPE OF REPORT & PERIOD COVERED: (9) Final rept. 1978-1979.
	6. PERFORMING ORG. REPORT NUMBER:
7. AUTHOR(s): (10) Michael K. Smith.	8. CONTRACT OR GRANT NUMBER(s): (12) 90
9. PERFORMING ORGANIZATION NAME AND ADDRESS: United States Naval Academy, Annapolis.	10. PROGRAM ELEMENT, PROJECT, TASK AREA & WORK UNIT NUMBERS
11. CONTROLLING OFFICE NAME AND ADDRESS: United States Naval Academy, Annapolis.	12. REPORT DATE: (11) 15 May 1979.
	13. NUMBER OF PAGES: 86
14. MONITORING AGENCY NAME & ADDRESS (if different from Controlling Office): United States Naval Academy, Annapolis.	15. SECURITY CLASS. (of this report): UNCLASSIFIED.
	15a. DECLASSIFICATION/DOWNGRADING SCHEDULE

16. DISTRIBUTION STATEMENT (of this Report) (14) USNA-TSPR-99

This document has been approved for public release; its distribution is UNLIMITED.

17. DISTRIBUTION STATEMENT (of the abstract entered in Block 20, if different from Report)

This document has been approved for public release; its distribution is UNLIMITED.

18. SUPPLEMENTARY NOTES

Accepted by the U.S. Naval Academy Trident Scholar Committee.

19. KEY WORDS (Continue on reverse side if necessary and identify by block number)

Alkaline-earth fluorides.
Calcium fluorides.
Defects.

20. ABSTRACT (Continue on reverse side if necessary and identify by block number)

It has become clear that simple point-defect models of relaxations in doped alkaline-earth fluorides are insufficient to explain experimental results. The idea that clusters of rare-earths may be associated with observed relaxations has been suggested. The writer attempted to study calcium fluoride crystals doped with two different rare-earth species, utilizing dielectric relaxation and ionic thermocurrent techniques to investigate the cluster hypothesis. If, in fact, a relaxation is associated with a dipolar cluster,

OVER

DD FORM 1 JAN 73 1473 EDITION OF 1 NOV 65 IS OBSOLETE S/N 0102-014-6601

UNCLASSIFIED.

SECURITY CLASSIFICATION OF THIS PAGE (When Data Entered)

245 600

JQB

hybrid relaxation involving both rare-earth species present should be observed.-- The finding (enclosed) provides useful new information concerning the defect structure of rare-earth doped calcium fluoride.--

0 - 0